

Technical University of Civil Engineering Geodesy Faculty

Thesis Scientific Report

The current state of multi-GNSS technology at international and national level

Phd student:

Eng. Andreea Mihăilescu

Scientific coordinator:

Professor, PhD, Eng. Iohan Neuner

2014-2015

CONTENTS

1.		Intro	oduct	ion to the current state of multi-GNSS technology at international and national level	3
2.		Pres	entin	g the current state of GNSS systems	4
	2.	1.	GPS	Architecture	4
		2.1.	1.	GPS Satellites	4
		2.1.	2.	GPS Signals	4
	2.	2.	Glor	nass architecture	6
		2.2.	1.	Satellites of the Glonass satellite system	6
		2.2.	2.	Glonass Signals	7
	2.	3.	Galil	eo system	8
		2.3.	1.	Galileo Satellites	8
		2.3.	2.	Galileo Signals	9
3.		Disc	ussin	g the problematics at IGS level	10
	3.	1.	Navi	gation Satellite Systems Status	11
	3.	2.	The	IGS Multi-GNSS Network	12
	3.	3.	Prec	ise orbits and satellite clocks	14
	3.	4.	Deve	eloping the Multi-GNSS concept in the near future	15
4.		Pres	enta	tion of international issues in various case studies	16
	4.	1.	Stud	y on the processing of GPS + Glonass data in the Asia - Pacific APREF network	16
	4.	2.	Prec	ise Point Positioning using Single-GPS and GPS + Galileo	22
	4.	3.	Mul	ti-GNSS RTK Positioning performance in New Zealand	27
		4.3.	1.	Introduction	27
		4.3.	2.	Multi-GNSS single-baselines functional models	29
		4.3.	3.	Multi-GNSS receiver used in the case study in New Zealand and Australia	30
		4.3.	4.	Results	31
5.		CON	ICLUS	SIONS	38
R	hli	oara	nhv		11

1. Introduction to the current state of multi-GNSS technology at international and national level

Completing the global positioning system with NAVSTAR-GPS satellites and with the GLONASS Russian positioning system in full operational phase as well as with the GALILEO European system in the partial operational phase expected by 2016 offers the opportunity to improve positioning accuracy using a combined positioning method.

GNSS systems are used in various applications: commercial, military, scientific; most applications can benefit from a combined positioning solution for GNSS systems. (J.Sanz Subirana 2013).

At international level, it is sought to improve positioning accuracy using GNSS technology by various methods, one of the current methods being the possibility of using a combined positioning technique of global positioning systems to achieve higher positioning accuracy, ensuring visibility in obstructed areas, DOP factor improvement.

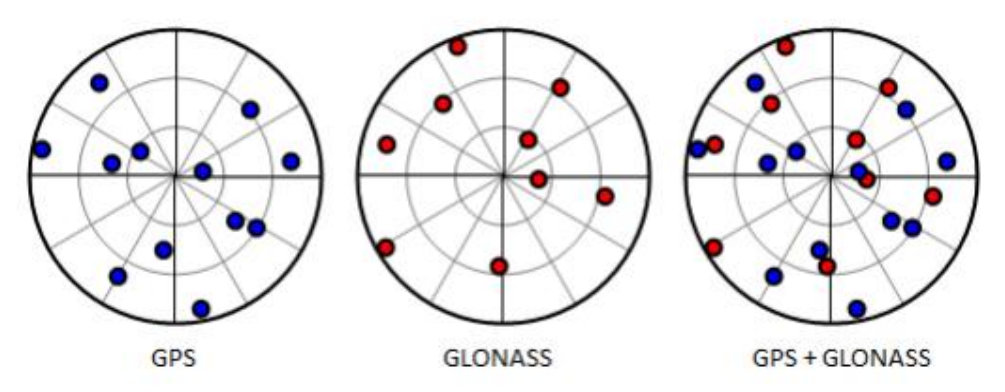


Fig.1.1. Sky plot for different GNSS configurations (Ferrao, 2013)

Global positioning systems have been designed to ensure compatibility and interoperability, features that make it possible to use multi-GNSS technology.

In recent years, many scientists have investigated the effect of combining GPS observations with GLONASS observations in the processing of the Continuous Operating Stations Network (CORS); additional observations have been designed to improve the authenticity of the network. At the 2011 IAG Symposium, a study was conducted to combine GPS observations with GLONASS within the Asian-Pacific Reference Network (APREF) with a minor contribution to the GLONASS segment. Nationally, GPS + GLONASS combined measurements have been carried out in isolated studies at permanent stations, concluding that GLONASS observations help to increase positioning accuracy to a small extent.

The degree of applicability is vast because in any position on the globe, a multi-GNSS solution can be adopted to enhance accuracy and resolve visibility problems with the relatively large number of satellites that will be visible from any position on Earth; the contribution of the GALILEO system being substantial as high since quality civilian applications will be available, services that are for only authorized users and military applications.

The purpose of this paper is to present a global positioning solution using a combined method of GNSS systems to achieve viable positioning accuracy. At the same time, positioning can be done with precision in obstructed vegetation environments, in densely built areas; the multipath effect is negligible, and the error due to the ionosphere is reduced.

Multi-GNSS special receivers are used to record mixed satellite signals that are transmitted at different frequencies, capable of ensuring data integrity, accuracy, high latitude performance, DOP factor improvement.

2. Presenting the current state of GNSS systems

2.1. GPS Architecture

2.1.1. GPS Satellites

The architecture of the GPS satellite system is based on the arrangement of satellites in blocks. Each block contains a set of satellites launched in orbit within a predetermined time frame.

- Block I, Navigation Development Satellites. Eleven satellites were launched between 1978 and 1985. These satellites were able to provide positioning information for 3 or 4 days without having contact with the control centre.
- Block II and II A, Operational GPS satellites. Since February 1989, 28 satellites have been launched, many of them are operational at present. Since 1990, satellites in Block II A (advanced) are operational. They are able to provide positioning information for up to 180 days without communicating with the control service.
- Block II R, Replacement Operational satellites. These satellites are able to determine their orbits and generate navigation messages. They are able to measure relative intersatellite distances and transmit information to other satellitesor to the control centre.
- Block II R-M, Modernised Satellites. These are the modernised satellites of II R block. The first satellite of this type was launched in September 2005. They can transmit on a new L2C civil signal and they include a new military signal.
- Block II F, Follow-on Operational Satellites. The first satellite of this type was launched in May 2010. They can also transmit on a new L5 frequency protected for safety-of-life applications. They also have inertial navigation systems.
- Block III. These satellites will enhance navigational capabilities, improving interoperability and resistance to signal jamming. They will provide the fourth civilian signal available on the L1 band (L1C). GPS satellites are identified in different ways: depending on the position in the orbital plane, according to the NASA reference number, or the Space Vehicle Number, etc.
- Full Operational Capability (FOC): GPS satellites reached this stage in March 1994 when the 24 Block II/IIA operational satellites were reached but was declared in July 1995. (Hoffman-Wellenhof, 2008)

2.1.2. GPS Signals

GPS signals are transmitted on two L-band radio frequencies reffered to as Link 1 (L1) and Link 2 (L2), respectively. They are circularly polarized and the frequencies are derived from a fundamental frequency generated by the atomic clocks onboard the satellites. $L_1 = 154 \times 10.23 \ MHZ = 1575.420 \ MHZ$

$$L_2 = 120 \times 10.23 MHZ = 1227.600 MHZ$$

Two services are active within the GPS satellite system:

- The Standard Positioning Service (SPS) service available on a wide users scale. It is a service that operates within the L1 frequency.
- The Precise Positioning Service (PPS) Service restricted to unauthorized access. It is only available to authorised users and military users.

The GPS system uses the CODE DIVISION MULTIPLE ACCESS (CDMA) technique to transmit different signals on the same radio frequency by modulation (Enge and Misra, 1999). The following types of codes and messages are modulated over the two carrier (L1 and L2):

- Coarse/Acquisition (C / A) code, also known as civilian code and defines SPS.
- Precision Code (P) is intended for military applications and is available to authorised civilian users. This code defines the PPS service.
- Navigation message D (t): It is modulated over both carriers' to provide information on ephemeris, satellite clock drift, ionospheric model coefficients, constellation status, among other information.

In order to restrict unauthorised access of civilians, the following measures were taken: S / A (selective availability) - deliberate degradation by manipulating the satellite clock, as well as ephemeris -; A / S (Anti - Spoofing) - encrypting the P code with a secret code W, resulting in the code Y modulated over the two L1 and L2 carriers.

In the figure below we can see the structure of the GPS satellite signal:

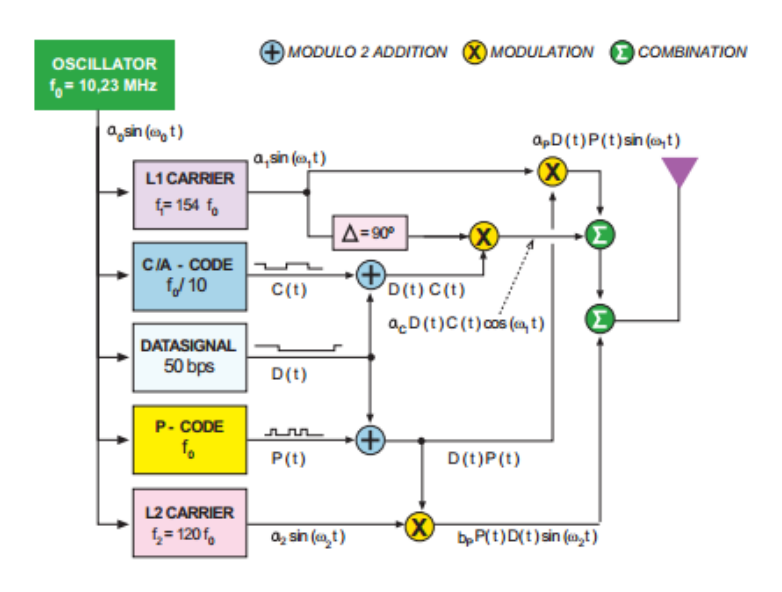


Fig.2.1 GPS satellite signal structure (Seeber 1993)

Tabel 2.1	. GPS	satellite	signal	structure	Seeber	1993)

Atomic clock frequency	$f_0 = 10.23 \text{MHz}$
Frequency L1	$154 \times f_0$
	1575.420 MHz
Wavelength L1	19.03 cm
Frequency L2	$120 \times f_0$
	1227.600 MHz
Wavelength L2	24.42 cm
P code frequency (chipping rate)	$f_0 = 10.23 \text{MHz} (\text{Mbps})$
P code wavelength	29.31 m
P code period	266 days, 7 days/satellite
C/A code frequency (chipping rate)	$f_0/10 = 1.023 \text{MHz}$
C/A code wavelength	293.1 m
C/A code period	1 ms
Navigation message frequency	50 bps
Frame length	30 s
Total message length	12.5 min

GPS Signal Modernisation. Introducing new signals.

Upgrading GPS signals involves the introduction of new L5 frequency signals as well as the introduction of new modulated codes on different frequencies - L2C, L5C and L1C - available to civilian users, as well as the Military Code M. Modernisation of the GPS system began in 2005 with the launch of the first Block IIR-M satellite. This satellite supported the new Military M signal, as well as L2C – civilian. The L2C civil signal has been specially designed to meet the needs of civilian users, as well as to develop the industry of two-way GPS receivers.

The plan for upgrading the GPS system continued with the launch of Block II F satellites that include, for the first time, the third civilian signal transmitted on the L5 band. This new L5C signal has another type of modulation. The next step involves Block III satellites including the fourth civilian L1 (L1C) civil signal capable of interoperability between the GPS system and other GNSS systems (such as Galileo). (ESA, 2013)

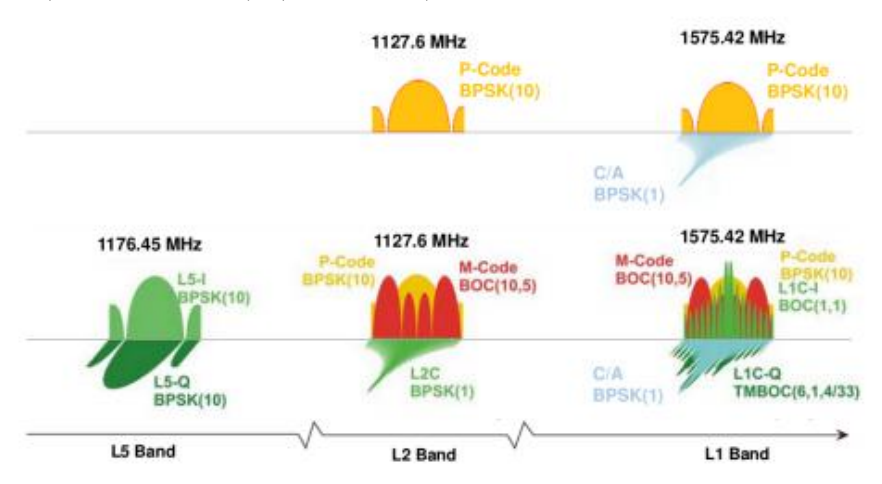


Fig.2.2. Spectrum of GPS signals before and after modernization (Courtesy of Stefan Wallner)

2.2. Glonass architecture

2.2.1. Satellites of the Glonass satellite system

Generations of the Glonass system:

- Prototypes (Generation Zero). The first prototypes of the Glonass (Uranus) satellites were launched in orbit in October 1982, with 18 launched satellites between 1982 and 1985, they are referred to as Block I satellites.
- First Generation. The first generation of Glonass satellites were based on the launch of satellites between 1985 and 1990. They are divided into different blocks (Block II a, Block II b and Block II v). They have improved time and frequency standards, improving frequency stability.
- Second Generation, called Glonass-M (Uragan M), a name that signifies an upgraded generation of satellites. They have been developed since 1990 with the first satellite launched in 2001. An impressive feature of these satellites is the introduction of a new civil signal on the G2 band that makes it possible to cancel the ionospheric refraction phenomenon.
- The Third Generation, called Glonass-K, makes it possible to access the new CDMA G3 on the G3 band, along with the civil signals on the G1 and G2 bands, and also have the Search and Rescue technique. The first satellite of this type was launched in February 2011.

• FOC (Full Operational Capability) was reached in December 2011. (ESA, 2013)

2.2.2. Glonass Signals

GLONASS signals are transmitted on two G-band radio frequencies transmitted on G1 and G2 frequencies.

Available Glonass services

- SPS The Standard Positioning Service is an open service available to users around the world. The navigation signal was initially provided only in the G1 frequency, but since 2004 the new Glonass-M satellites transmits a new civil signal on the G2 frequency.
- PPS The Precise Positioning Service is available only to military and licensed users. Two navigation signals are available in the G1 and G2 bands.

Each Glonass satellite transmits on a certain frequency within the band. This frequency determines the frequency channel number and allows receivers to identify satellites using the FDMA technique. Upgrading the Glonass signals makes it possible to transmit the CDMA signals on the G1, G2, G3 (L3) bands, and on the L5 GPS band in order to transmit the FDMA signals to the G1, G2 bands.

The frequencies to which the Glonass G1 and G2 signals are transmitted are determined by the channel number k:

G1:
$$f_1(k) = 1602 + k \times \frac{9}{16} = (2848 + k) \times \frac{9}{16}MHZ$$

G2:
$$f_2(k) = 1246 + k \times \frac{7}{16} = (2848 + k) \times \frac{7}{16}MHZ$$

The numbers corresponding to the frequencies f are taken into consideration for the supply of 24 channels, $k=1,\ldots,24$. Taking into account the directives issued by the International Union of Communications on Electrical Basis, all Glonass satellites launched after 2005 were forced to use a number $k=-7,\ldots,6$. This change is intended to avoid interference with radio astronomy frequencies and satellite communications services.

Reducing the number of channels from 24 to 12 is compensated internally because two satellites located on the same orbit transmit exactly on the same frequency but occupy diametrically opposed positions. Consequently, they will not be recorded at the same time by a ground receiver (but the space stations will have to implement functions to distinguish between the two satellites).

These frequencies modify the C / A and P codes together with the navigation message D. The transmitted codes have a twice as great noise as the GPS.

As with the GPS, the C / A code was modulated only on the G1 frequency, while the P code was modulated on both the G1 frequency and the G2 frequency, the new Glonass type M (Upgraded) satellites transmit the C signal / A and frequency G2. The receiver therefore identifies the satellite according to the frequency at which the signal is emitted.

S / A is not applied to the Glonass satellite system and also the P code is not encrypted.

Glonass Signal Modernisation. Introducing new signals and CDMA usage technique.

In the modernization of the Glonass signals, the implementation of a new GLONASS-K G3-specific frequency was envisaged. This signal will generate a new C / A2 civilian code, as well as a new P2 military code for Safety Of Life (SOL) applications.

The addition of the CDMA technique as well as the FDMA was possible with the release of the Glonass-K satellites in fever 2011, providing CDMA signals at a frequency band G3 close to the Galileo-specific E5b frequency.

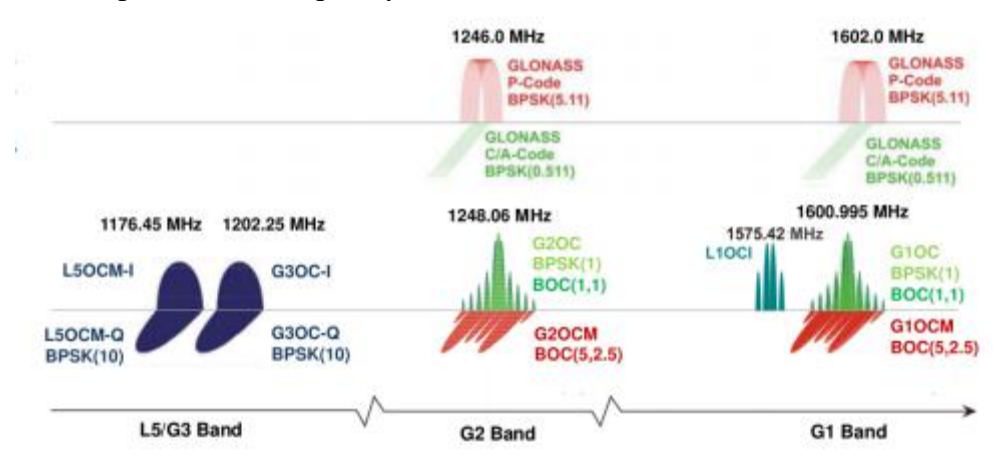


Fig.2.3 Spectrum of Glonass signals. FDMA signals before and after upgrading (at the top), as well as displaying new CDMA signals after upgrading (at the bottom). (Courtesy of Stefan Wallner)

Band	Carrier freq.	PRN	Modulation	Code rate	Data rate	Convice
Danu	(MHz)	code	type	(Mcps)	(bps)	Service
G1	1602.0000+	C/A	BPSK(0.511 Mcps)	0.511	50	Civil
GI	+0.5625k	Р	BPSK(5.11 Mcps)	5.11	50	Service
G2	1246.0000+	C/A	BPSK(0.511 Mcps)	0.511	50	Civil
62	+0.4375k	Р	BPSK(5.11 Mcps)	5.11	50	Military Civil

Tabel.2.2. The Glonass System Signals. (ESA, 2013)

2.3. Galileo system

2.3.1. Galileo Satellites

- Experimental Phase Two GIOVE (Galileo In-Orbit Validation) GIOVE (GIOVE A and GIOVE B) experimental satellites were launched in 2005-2008. They were launched to answer several questions: the affiliation of the transmission of signals at different frequencies to the Union The International Telecommunications Authority, in order to validate the environmental monitoring technologies used in Galileo's operational constellations and generate signals capable of being received by special receivers. Both satellites were created in parallel to answer questions about orbital redundancy as well as to provide complementary capabilities.
- IOV Phase. At this stage, ground tests are performed. In this phase, four IOV satellites have been launched. The first two satellites were launched in October 2011, being placed in the first orbital plane. The second pair of satellites was launched one year away, being placed in the second obital plane.

• FOC Phase. By 2014-2016, the Galileo constellation is expected to reach 18 satellites, including the four IOV satellites, and the FOC phase is expected to be reached between 2019-2020 reaching a constellation of 27 satellites and three replacement satellites. (ESA, 2013)

2.3.2. Galileo Signals

In FOC Phase each Galileo satellite transmits 10 navigation signals on frequencies E1, E6, E5a, E5b. These signals are capable of being accessible to Galileo and EGNOS such as:

- OS (The Open Service) available to users around the world. Up to three separate frequencies are available. The single-frequency receivers performance will be similar to the C / A GPS receivers. In general, OS applications use a combination of GPS signals and Galileo to improve positioning accuracy in difficult environments such as urban areas.
- PRS (The Public Regulated Service) is a service designed for local authorities (police, military agencies) with government-controlled access. Enhanced signal modulation/encryption is introduced in order to be robust.
- CS (The Commercial Service) is an available service protected by commercial encryption.
- SAR (Search and Rescue Service) contributes to Cospas-Sarsat international service. A
 signal characteristic of this service will be retransmitted to the Rescue Coordination
 Centre and Galileo System will be able to inform users that their situation has been
 detected.
- SoL (The Safety-of-Life Service) is available for aviation applications and due to EGNOS the performance of the service will always be improved. (ESA, 2013)

Similar to GPS satellites, all satellites share the same frequencies and the signals are differentiated by the CDMA technique (Galileo SIS ICD, EU, 2010).

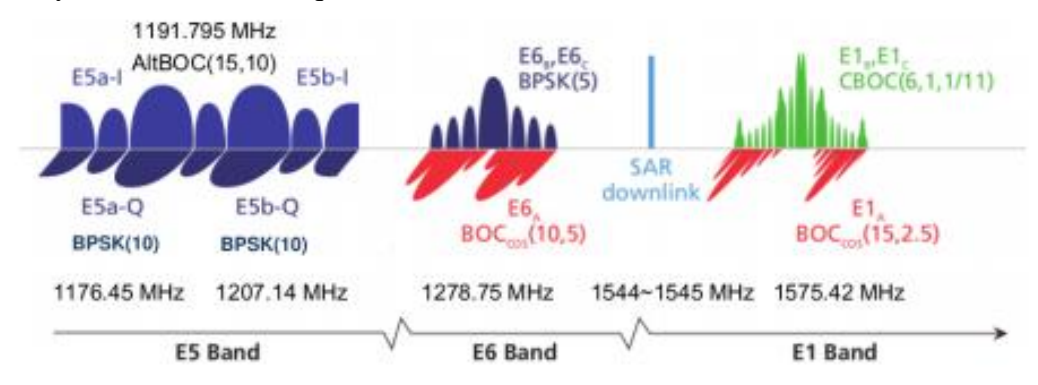


Fig. 2.4. Spectra of Galileo system signals (Courtesy of Stefan Wallner)

The E1 signal supports the OS, CS, SoL, and PRS services. It contains three navigation signals modulated on the L1 band. E1-A is encrypted and available to PRS users only, containing PRS data. The E1-B and E1-C components are available to civilian users with unencrypted codes. E1-B is a data channel, and E1-C is a pilot channel (data less channel).

E6 signal is dedicated to CS and PRS services. It consists three navigation patterns modulated on the E6 lane. E6-A is encrypted only for PRS users. E6-B and E6-C are accessible and commercially available (CS) and include a data channel and a pilot channel. The codes are encrypted on the E6 frequency, and it is similar to Beidou's B3 band.

E5a supports the open service. Includes two E5a-I components (including data) and E5a-Q. On this frequency, positioning information is transmitted (note that this frequency overlaps the GPS L5, the Beidou B2a and future Glonass L5 signals).

E5b supports OS, CS, and SoL. It is an open access ignal to users transmitted in the E5b-I components (including data) and E5b-Q (this signal is common BeiDou B2b as well as Glonass G3).

The E5a and E5b components are modulated onto a single E5 frequency and can be processed together as a single signal with a specific receiver, reducing the effect of multipath and noise. (ESA, 2013).

3. Discussing the problematics at IGS level

With four new satellite systems (BeiDou, Galileo, QZSS, IRNSS) along with existing satellite systems in the modernization phase (GPS, GALILEO), the class of space satellite systems is undergoing a change phase. The International GNSS Service (IGS) has initiated the Multi - GNSS Experiment service to enable the user to familiarize themselves with the new satellite systems as well as prepare their incorporation into a high - precision global satellite modeling and analysis.

Over the last decade, satellite positioning systems have undergone a major change phase. Starting from a GPS satellite positioning system consisting of a single constellation, a set of six global or regional satellite systems - GLONASS, BeiDOU, Galileo, the Quasi-Zenith Satellite System (QZSS) and the Indian regional satellite system (IRNSS), spatial systems offer the opportunity to create a space-based and time-based position (PNT) service.

These services are complemented by augmented spatial systems (SBAS) to enhance availability, accuracy of positioning, navigation and timing for safety applications.

The high potential of satellite positioning systems developed so far has led to a combined use of these to enhance positioning accuracy using multiple signals compared to a GPS standalone positioning system. The new signal structures will be robust in order to avoid the interference phenomenon and the multipath effect, but will also be able to track at low signal levels.

The availability of unencrypted signals enables on three frequencies enables new approaches to determine ambiguities in the relative GNSS differential positioning with carrier-phase-based observations and at the same time provides considerable precision in determining the delay due to the ionosphere.

Ultimately, increasing the number of satellites not only greatly improves accuracy in satellite positioning applications, but also provides an increased number of satellite signals for spatial meteorological applications, which implies recording the ray of the neutral atmosphere and the ionosphere.

Given the remarkable contributions of satellite systems to science and Geodesy, similar contributions are also expected from positioning, navigation and timing services (PNT).

With the implementation of GPS signals in the upgrading and augmentation of GNSS space systems as well as augmentation systems (Russian Differential Correction and Monitoring System - SCDM and Geoscience Indian GAGAN Augmentation System), IGS wants to grow in the multi-branch-GNSS to optimize a multi-GNSS service that users can manipulate.

IGS initiated the Multi-GNSS Experiment (referred to as MGEX) under coordination of its Multi-GNSS Working Group. MGEX serves as a framework for increasing the overall awarness of multi-GNSS within engineering communities and scientists, and at the same time

ensure the familiarity of IGS members and users with the new navigation satellite systems. (IGS - MGEX, 2014).

3.1. Navigation Satellite Systems Status

In the table below, information on PNT systems and operational satellites can be observed according to the latest information available from IGS - MGEX. Global Positioning Systems GPS and GALILEO have reached the full operational phase and provide signals on at least two frequencies (L1, L2) accessed by civilian users.

The last generation of the US GPS GPS II F satellites and the Russian K type satellites offer a new frequency (L5 or L3), but these signals are limited to a small number of users. (IGS - MGEX, 2014)

Tabel 3.1: Status of global and regional navigation satellite systems as of September 2013

System	Blocks	Signals	Sats
	IIA	L1 C/A, L1/L2 P(Y)	8
GPS	IIR-A/B	L1 C/A, L1/L2 P(Y)	12
	IIR-M	+L2C	7
	IIF	+L5	4
GLONASS	M	L1/L2 C/A + P	24
GLUNASS	K	+L3	(1)
	GEO	B1, B2, B3	5
BeiDou	IGS0	B1, B2, B3	5
	MEO	B1, B2, B3	4
Galileo	10V	E1, (E6), E5a/b/ab	(4)
QZSS	n/a	L1 C/A, L1C, SAIF L2C, E6 LEX, L5	1
IRNSS	n/a	L5,5	(1)

In addition to GPS and GLONASS satellite systems, BeiDOU system offers a standalone navigation service fot the China and Asia Pacific area with a global service expected to be available by 2020. Although the BeiDOU Open Service Interface Document Control (ICD) Service provides coverage on the two B1 and B2 signals, a multi-GNSS positioning will be reached when up to three frequencies are available. Therefore, BeiDOU is the first satellite navigation system to offer an improved positioning method with the use of three frequencies.

GALILEO has four IOV satellites (In Orbit Validation) that have not been operational until now. Two pairs of satellites from the Full Operability Capability Phase (FOC FM) were launched during the operational year 2015. Global GALILEO operational service is expected to be active in the coming years. Access to the E6 frequency is not completely defined, users can

access the signals on E1, E5a / E5b frequencies with advanced performance in annihilating the multipath effect.

GALILEO satellites are equipped with a passive hydrogen masers that provides stability to atomic clocks, leading to many benefits for real-time applications, precise positioning and scientific applications.

Japan has validated the QZSS concept, starting from an operational satellite. The full operational phase embedding 3 satellites in inclined geosynchronous orbit (IGSO) is expected to be reached in the coming years of this decade. QZSS consists of a number of unique satellite signals distributed over four frequencies and provides different types of corrections for different types of users from an intermediate level of training to advanced.

India launched the IRNSS -1 satellite in July 2013, IRNSS -1 B in April 2014, IRNSS - 1 C in October 2014, and IRNSS 1 - D in March 2015. It is expected to have four satellites disposed in inclined geosynchronous orbits IGSO) and 2 geosynchronous satellites (GEO). IRNSS -1 transmits signals on L5 and S frequencies, so common GNSS receivers can not capture information due to lack of information on the L5 frequency and the need for a second common frequency.

The six navigation satellite systems are complemented by a total of 13 SBAS systems with constellations distributed in geostationary orbits. A growing number of SBAS-type augmentation systems provide two L1 / L5 ranging signals that can be recorded by modern GNSS receivers and can be developed in the field of precise positioning applications. (IGS - MGEX, 2014)

3.2. The IGS Multi-GNSS Network

A multi-GNSS network has been developed by IGS distributed across the globe in the development of existing ones (GPS and GLONASS), and based on information obtained from national agencies, universities, 90 stations have been built into the M-GEX network to which 10 stations were added to the Asia Pacific region, reaching 125 stations, and in September 2015 the network was integrated into the IGS network.

MGEX incorporates resources from institutions that have upgraded their GNSS monitoring network networks or set up new multi-GNSS monitoring stations capable of recording multiple signals. MGEX is based on a heterogeneous global network that embraces large-scale equipment for users. The most common receivers are included in the Manufacturers section. Most sites employ choke-ring antennas, but mostly *grade* antennas are used.

Although the variety of receivers and antennas implies a challenge in data processing, this variety also implies a great advantage. The diversity of satellite signal recording techniques and the types of data employed by the various receivers contributes to a better understanding of the new satellite signals. At the same time, the differences between different types of equipment contributes to the improvement of the GNSS receivers. (IGS - MGEX, 2014)

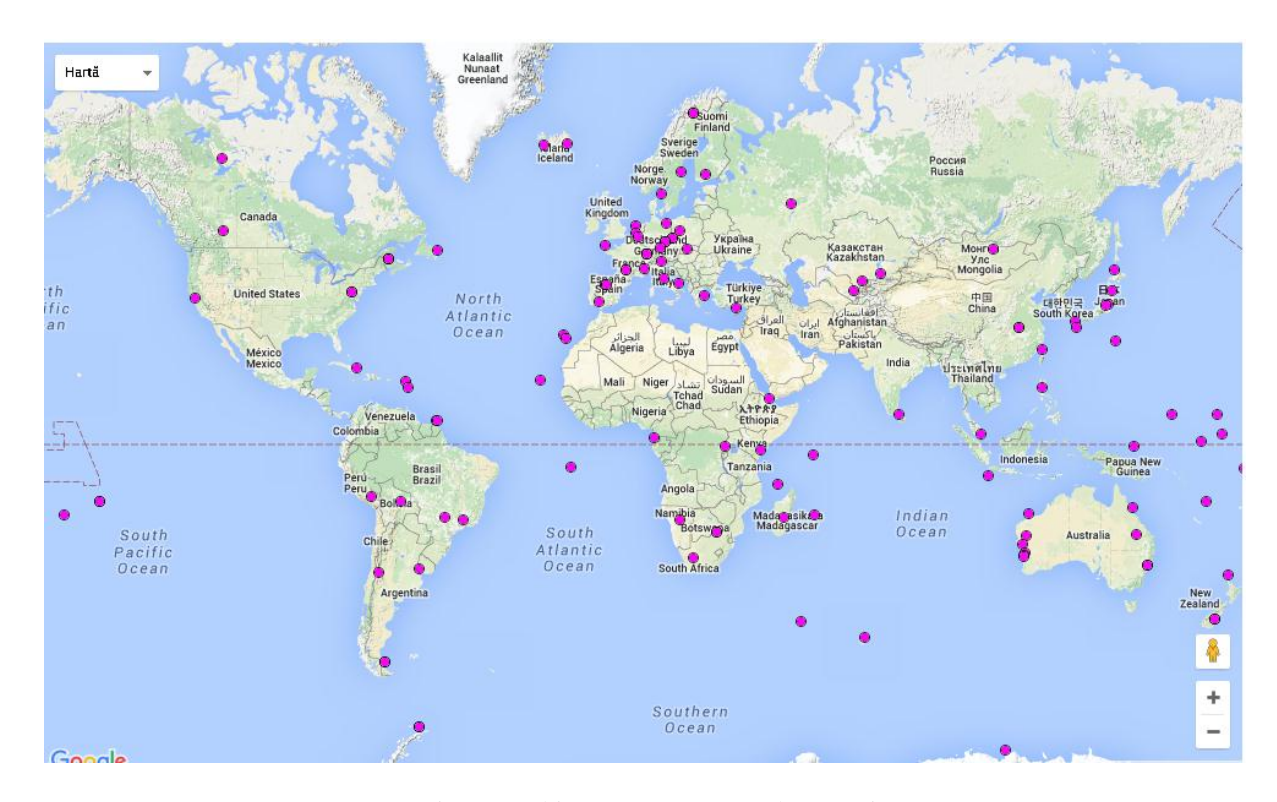


Fig 3.1 Multi-GNSS IGS Network (www.igs.com)

In July 2015, IGS succeeded in integrating corrections into antenna phase center modeling within newly developed satellite systems (Galileo, BeiDou, QZSS, IRNSS) available for the following antennas:

Tabel 3.2 Antenna phase center variation corrections (www.igs.com)

Satellite Antennae IGS Codes-20 columns XXXXXXXXXXXXXXXXXX	Description Description
BEIDOU-2G /	BeiDou-2 GEO
BEIDOU-2I	BeiDou-2 IGSO
BEIDOU-2M	BeiDou-2 MEO
BEIDOU-31	BeiDou-3 IGSO
GALILEO-0A	Galileo In-Orbit Validation Element A (GIOVE-A)
GALILEO-0B	Galileo In-Orbit Validation Element B (GIOVE-B)
GALILEO-1	Galileo IOV : GSAT 0101-0104
GALILEO-2	Gatiteo FOC : GSAT 0201-0222
IRNSS-1GEO	IRNSS-1 GEO
IRNSS-1IGSO /	IRNSS-1 IGSO
QZSS I	QZSS : SVN 01

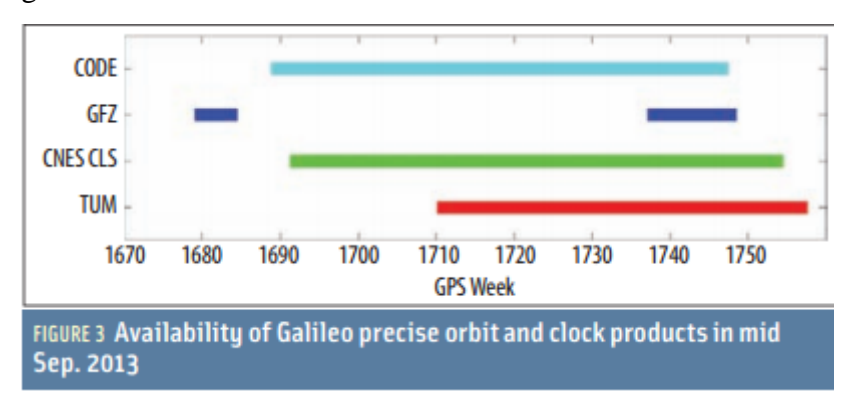
MGEX uses data from NASA, the French Institut Geographique National (IGN), and the BKG archive to obtain satellite data, as well as to distribute the satellite orbit parameters collected by the MGEX network. To facilitate these activities, the RINEX 3 format (Receiver Independent Exchange Format 3) was adopted. The introduction of extended data storage formats is planned at a stage where MGEX users are coordinating with IGS infrastructure.

Other formats for presenting satellite data besides the RINEX or RTCM format have been created, namely the MSM format whose messages can be plated on all satellite constellations, satellite signals and observations to provide full compatibility with the information contained in the RINEX files. (IGS - MGEX, 2014)

3.3. Precise orbits and satellite clocks

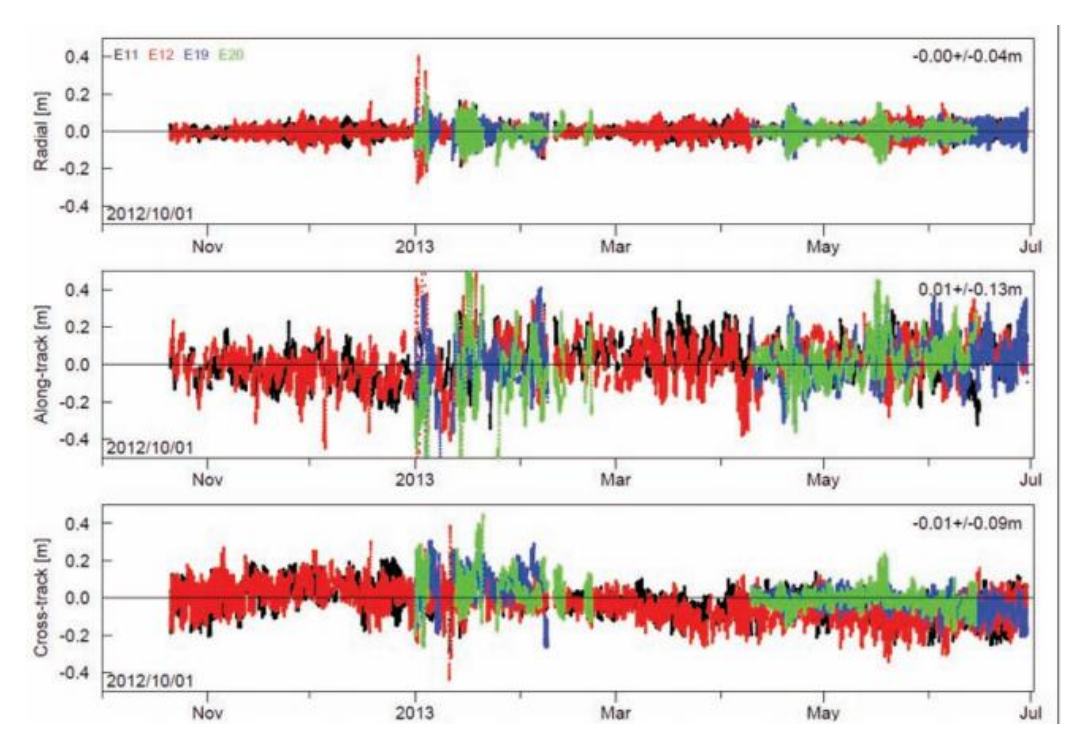
As a first step in integrating new satellite constellations within a multi-GNSS IGS service, space institutions provides orbits and accurate clocks for Galileo, QZSS based on information from the MGEX network and other GNSS stations. The data is available to interested users and can be found in the MGEX archive being maintained by CCDIS. Similar data is also expected to be obtained for BeiDou.

Galileo. Technical University of Munich (TUM) and CNES provide data on satellite orbits and clocks products for the four Galileo IOV satellites and for FOC every three to six days. Ephemerides are post-processed using the information obtained from the Orbit Determination Center in Europe (CODE). The oblivion calculated by MGEX, as well as the satellite clocks cover a period of up to one-half years, which leads to a long-term performance satisfying a wide range of conditions.



Fig, 3.2. Availability of Galileo precise orbits and clock products in September 2013 (IGS - MGEX, 2014)

Figure 3.2 demonstrates the difference between the orbital estimates offered by TUM and CODE. Making an arithmetic average of all satellites over eight months, the two products record a difference of about 16 cm (in 3D positioning), which implies a 5 cm orbital uncertainty. Orbital estimates given by CNES and CLS give a threefold error.



Fig, 3.3. Differences of MGEX precise orbit products for the Galileo IOV satellites (IGS - MGEX, 2014)

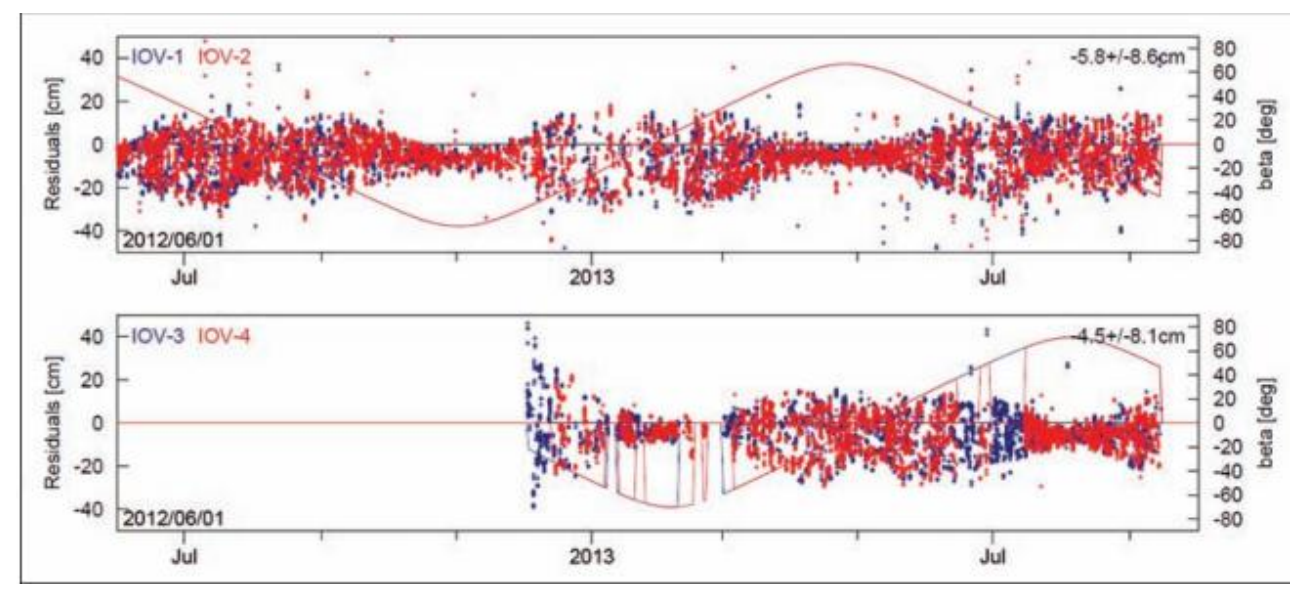


Fig 3.4. The results obtained with the SLR CODE and TUM technology for the two Galileo IOV satellite pairs. Solid lines signify the Sun angle above the orbital plane (β angle). (IGS - MGEX, 2014)

3.4. Developing the Multi-GNSS concept in the near future

The creation of the MGEX network has laid the foundation for an early familiarization with new GNSS systems and signals. The first steps have been made by providing precise orbits information for individual GNSS system and integrating MGEX into the IGS network. It is expected that key objectives to be pursuated:

- The expansion of multi-GNSS within the frame of overall IGS network;
- The consideration of additional constellations (BeiDou, IRNSS, and, optionally SBAS augmentation systems) in the precise ephemeris generation;

- Development of a new multi-GNSS / multi-signal within data processing and ionosphere modeling;
- Characterization of the new GNSS satellites and the development of common processing standards for orbits and clock products;
- Development of quality control of the multi-GNSS / multi-signal (within noise errors, cyce slip, satellite signal reflection) extended to the entire network.

The development of the MGEX network focuses on the incorporation of satellite constellations and on an improved description of the space and land segment. (IGS - MGEX, 2014)

4. Presentation of international issues in various case studies

4.1. Study on the processing of GPS + Glonass data in the Asia - Pacific APREF network

In various specialized works, the impact of multi-GNSS technology on improving 3D positioning accuracy is studied.

From 2009 to April 2011, there was an improvement in the positioning accuracy of the permanent stations using the Glonass observations. Due to the fact that the Glonass Russian positioning system was not fully functional at that time, reaching the constellation of 24 satellites distributed on 3 orbital planes in December 2011, it was concluded that the improvement in positioning accuracy is up to 30%.

Although the constellation of the Glonass system was not fully operational with a smaller number of satellites (2-3 mean), the Glonass observations helped improve positioning accuracy based on improved satellite geometry. These improvements are important in cinematic applications, in obstructed areas of low visibility vegetation, in densely built areas, canyons, mountainous areas.

Curtin University has been working as Local analysis Centre for APREF network since January 1, 2009 together with Geoscience Australia, with the aim of providing weekly coordinates and ZTDs (Zenith Tropospheric Delays) estimates for an APREF sub-network.

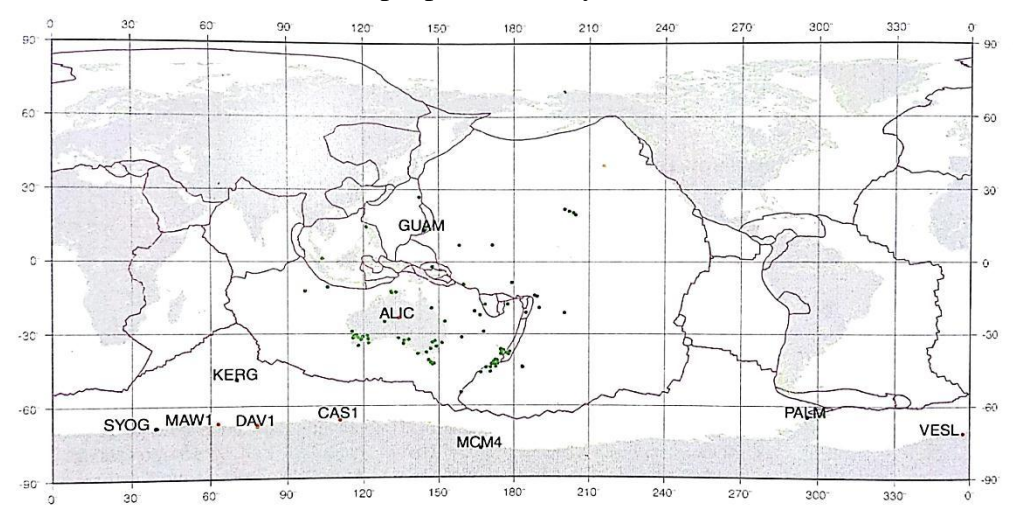


Fig. 4.1. – The cluster of APREF stations processed by CU LAC since Jan 2011. Symbolization: Red dots -GPS stations + GLONASS, Blue dots - GPS-only stations. (A. Nardo, 2011)

With the help of the compensation software, the phase observations (which ensure the formation of double difference equations) were processed daily based on a processing scheme. [Beutler et al. 2007].

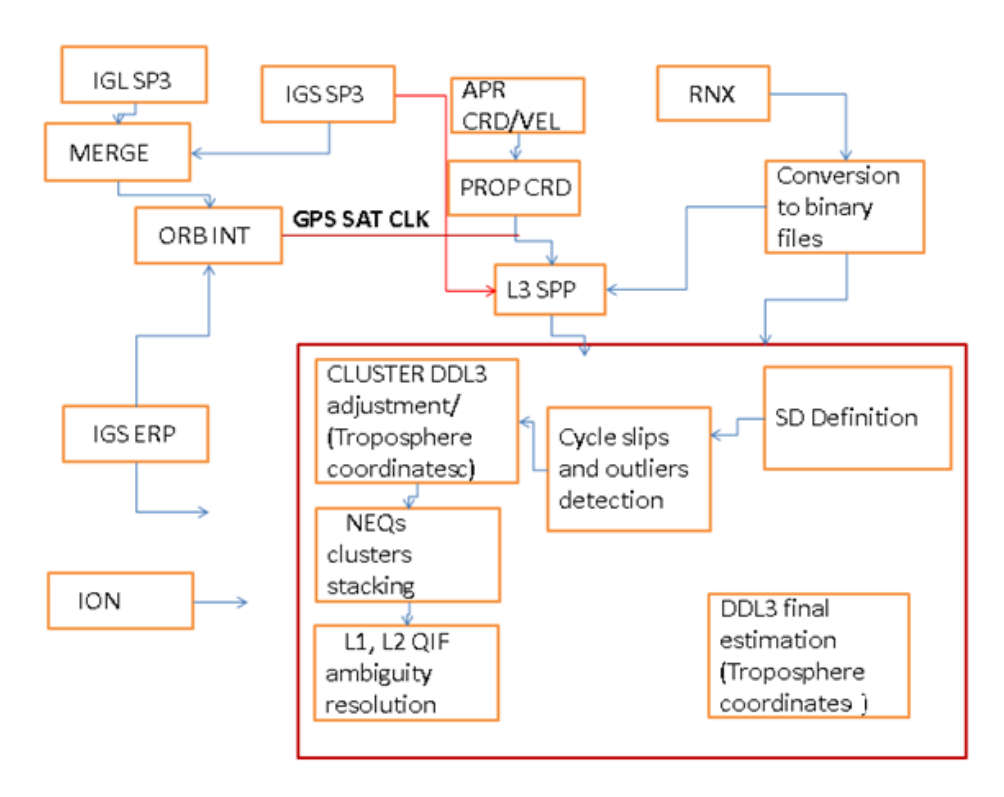


Fig.4.2 – Processing strategy used for combined GPS + GLONASS processing combined observations (A. Nardo, 2011)

Generally in relative precision (centimeter) positioning, phase observations are used. The most used processing techniques are those in which equations of simple, double and triple differences are generated between the initial (undifferentiated) observation equations.

Each daily session of measurements was processed in parallel using the strategy illustrated in Figure 4.2. The strategy involves four steps: (1) Data Preparation (data download, reformatting of the files), (2) Data editing (synchronization of receivers clocks, cycle slip detection, estimation of a first approximation solution), (3) Ambiguity Resolution (4) Final adjustment.

The GPS IGS and the GLONASS (IGL) were merged into one file (box MERGE), and the scheduling of the receiver's clock was performed using GPS codes. For each daily session of satellite observations, bases have been defined to maximize GPS observations.

A float double differenced solution, based on the ionosphere free model, was obtained by processing a group of five individual stations and combining the normal group equations to determine an approximate solution of the network. The ambiguities are fixed by integer values based on the Quasi Ionosphere Free model. Each base is processed separately, keeping fixed the ZTDs and the coordinates of a single station estimated in the float solution.

No attempt has been made to estimate GLONASS ambiguities because the ambiguity determination strategy used (SIGMA Beutler et al., 2007) can be applied only for short baselines (not exceeding 20 km).

The final estimates, based on a sample of 180 data, are the daily coordinates and ZTDs values (2 h sampled) (box DDL3 final estimation).

The high number of satellite observations due to the inclusion of GLONASS observations should have a contribution in estimating station coordinates as well as in ZTDs determination, but this improvement is reduced by an increase of the number of parameters to be estimated, mainly the GLONASS float ambiguities.

Taking into account long-term processing, coordinate estimates are taken into account by two daily processings (GPS and GPS + GLONASS) in order to evaluate the possible accuracy improvement (i.e. the standard deviations of the coordinates). The results are reported for stations located in Antarctica (seven stations in total), Australia and the other 2 stations located on the edge of the APREF network, in order to emphasize the possible effect of the better observation geometry due to GLONASS orbit inclination at high latitudes.

Table 4.1. CU-specific values during the first 160 days of 2010 (A.Nardo, 2011)

Total num. of receivers	84
Num. of observed GPS satellites	31
Fract. of fixed GPS amb. per day	0.83
Ratio between GPS-only and GPS + GLO rec.	0.6
Num. of ZTDs values per rec. per day	13
Average num. of epochs per sat. pass (180 s sampl.rate)	130
Average num. of cycle slips per pass	3

The time series obtained from daily records are used to express the accuracy (repeatability) of the coordinates. The CATREF software (Altamimi et al., 2007) has been used for stacking time series, the mathematical model otherwise solves the problem of both coordinates and the parameters of the reference network, removing the effect due to the variability of the reference frame definition from the coordinates time series.

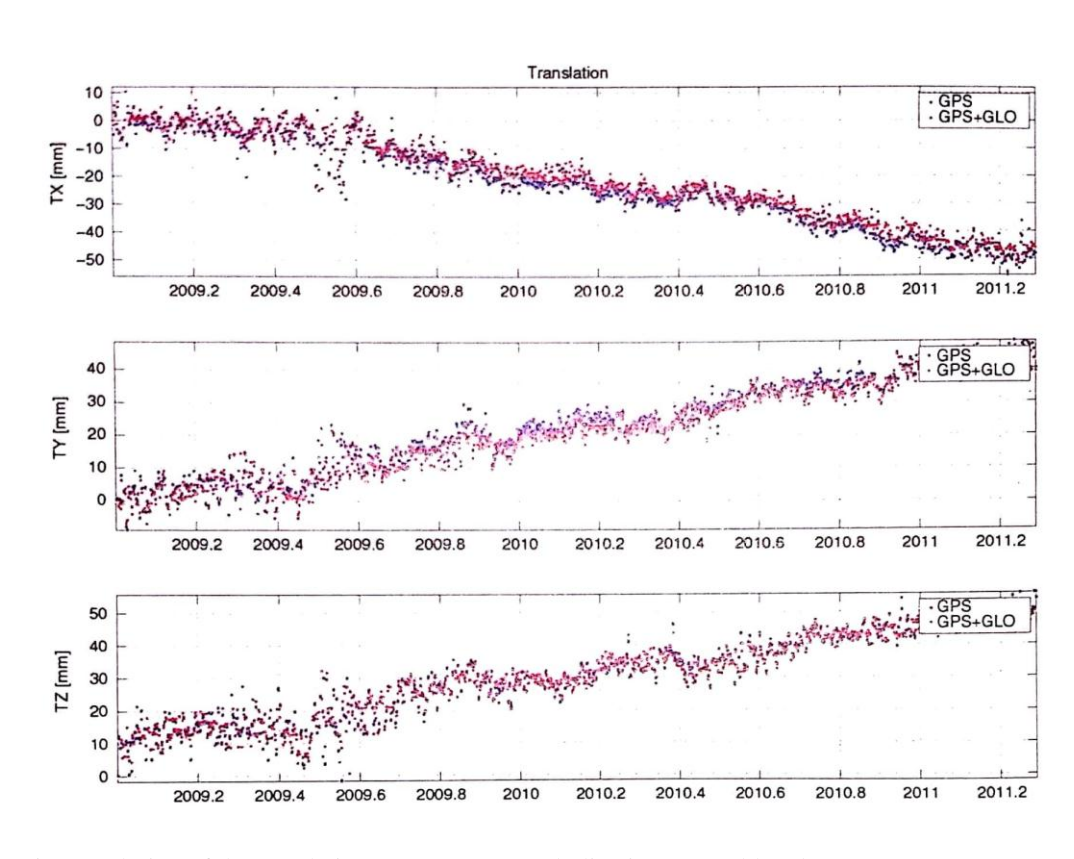


Fig.4.3 – Time evolution of the translation parameters. Symbolization: GPS (blue dots), GPS + GLONASS (red dots) (A. Nardo, 2011)

The CATREF functional model is based on (linearized) coordinates and velocity transformations between two or more reference frames. The approximate coordinates and velocities stored in the SINEX files together with the corresponding variance-covariance matrix (VCV) can be used as observations in least squares compensation after the initial constraint is removed.

Considering that each set of coordinates (each SINEX file) defines another reference frame and also taking into account the coordinates and the velocities of the sites, the software estimates the 14 Helmert parameters (translation, rotation, scale factor and their time derivatives) between two reference frames as well as the coordinates and the velocities in a combined reference frame. The time-dependence of the Helmert parameters can be considered linear (as can be seen in Figure 4.3.).

The linearized observations equations can be expressed as:

$$X_{S}^{i} = X_{C}^{i} + (t_{S}^{i} - t_{0})\dot{X}_{C}^{i} + T_{k} + D_{k}X_{C}^{i} + R_{k}X_{C}^{i} + (t_{S}^{i} - t_{k})[\dot{T}_{k} + \dot{D}_{k}\dot{X}_{C}^{i}]$$

$$\dot{X}_{S}^{i} = X_{C}^{i} + \dot{T}_{k} + \dot{D}_{k}X_{C}^{i} + \dot{R}_{k}X_{C}^{i}$$

$$(4.1)$$

With X_S^i şi \dot{X}_S^i are denoted the coordinates, respectively the velocity for each individual solution S şi and for each station i at epoch t_s^i in a given reference frame (TRF) k; X_C^i şi \dot{X}_C^i and represents the coordinates and the velocity in the combined reference frame, t_k tk is the epoch each TRF refers to; T_k , D_k , R_k represents the translation, rotation and scale factor, \dot{T}_k , \dot{D}_k , \dot{R}_k are their time derivatives; t_0 being is a reference epoch..

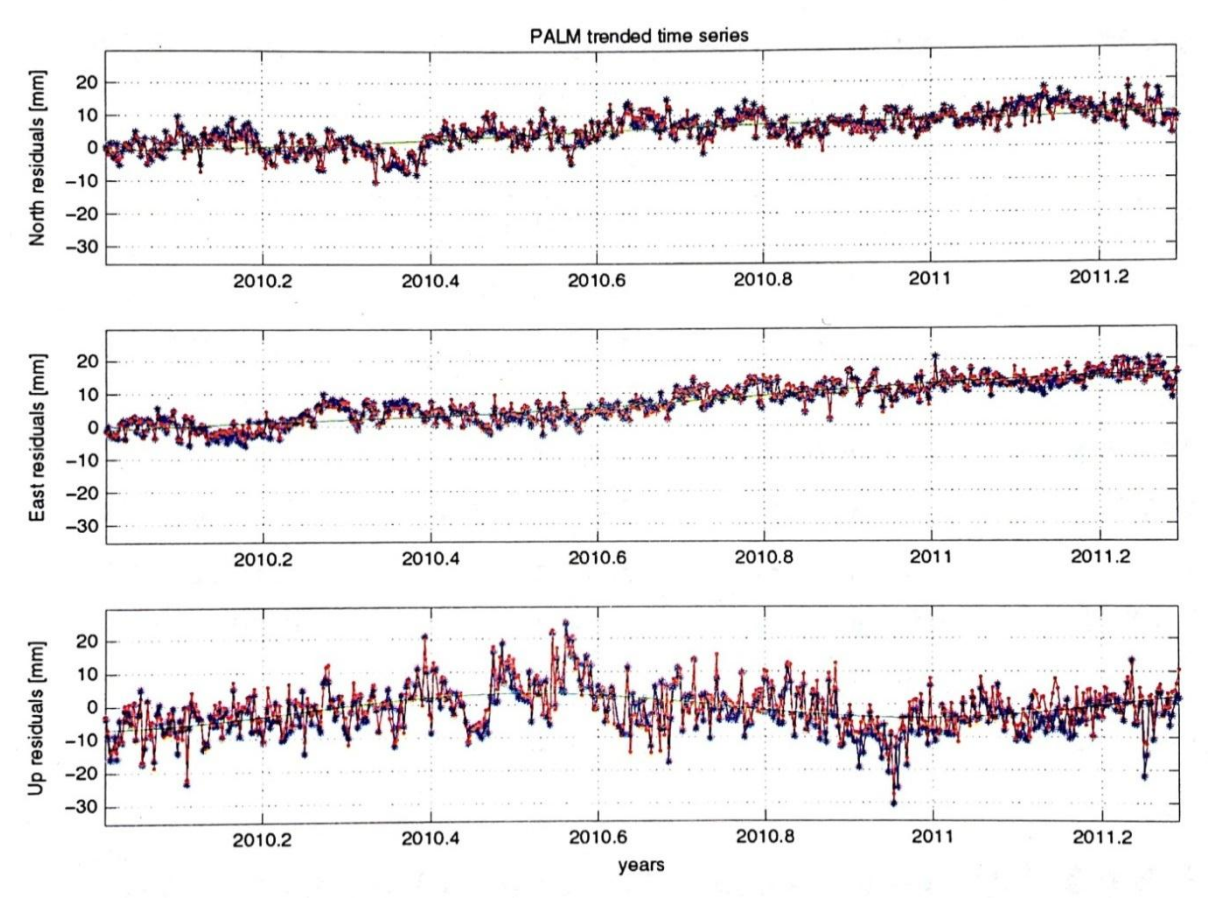


Fig.4.4 – Example of a time series that highlights a secular and periodic motion (PALM station), the green line represents the adjusted model. (A. Nardo, 2011)

For the considered sites, the empirical variance-covariance matrices have been computed by meand, and the corresponding standard deviations have been estimated. In order to evaluate the improvement of the GPS + GLONASS positioning accuracy processing compared to GPS –only processing, it is defined the non-dimensional quantity Fi:

:

$$F_i = 1 - \frac{\hat{\sigma}_i^{GPS+GLO}}{\hat{\sigma}_i^{GPS}}, i = n, e, u \tag{4.2}$$

Fi is positive and smaller than 1 if the additional GLONASS observations improve the estimate of the unknown parameters, otherwise it is negative. Table 4.2 centralizes the results of the comparison: as can be seen, the GLONASS system does not give a remarkable improvement; also there is no remarkable effect dependent on the latitude of the sites of stations.

Table 4.2 Standard deviations with their precision for the considered stations (mm) GPS-only case (A. Nardo, 2011)

Site	$\hat{\sigma}_n$	$\hat{\sigma}_e$	$\hat{\sigma}_u$
MCM4	2.48 ± 0.02	2.38 ± 0.02	8.37 ± 0.02
VESL	3.23 ± 0.03	3.11 ± 0.03	5.82 ± 0.03
SYOG	3.01 ± 0.03	3.26 ± 0.03	4.96 ± 0.03
DAV1	2.62 ± 0.03	2.89 ± 0.03	4.73 ± 0.03
MAWI	2.76 ± 0.03	2.99 ± 0.03	5.01 ± 0.03
CASI	2.54 ± 0.03	2.47 ± 0.03	4.56 ± 0.03
PALM	4.42 ± 0.03	3.43 ± 0.03	7.09 ± 0.03
KERG	3.82 ± 0.03	3.33 ± 0.03	3.91 ± 0.03
ALIC	1.28 ± 0.03	1.25 ± 0.03	5.68 ± 0.03
GUAM	2.83 ± 0.03	4.52 ± 0.03	10.81 ± 0.03

Table 4.3 Standard deviations with their precision for the considered stations (mm)

GPS + GLONASS case (A. Nardo, 2011)

Site	$\hat{\sigma}_n$	$\hat{\sigma}_e$	$\hat{\sigma}_u$
MCM4	2.48 ± 0.02	2.38 ± 0.02	8.37 ± 0.02
VESL	3.23 ± 0.03	3.11 ± 0.03	5.82 ± 0.03
SYOG	3.01 ± 0.03	3.26 ± 0.03	4.96 ± 0.03
DAV1	2.62 ± 0.03	2.89 ± 0.03	4.73 ± 0.03
MAWI	2.76 ± 0.03	2.99 ± 0.03	5.01 ± 0.03
CASI	2.54 ± 0.03	2.47 ± 0.03	4.56 ± 0.03
PALM	4.42 ± 0.03	3.43 ± 0.03	7.09 ± 0.03
KERG	3.82 ± 0.03	3.33 ± 0.03	3.91 ± 0.03
ALIC	1.28 ± 0.03	1.25 ± 0.03	5.68 ± 0.03
GUAM	2.83 ± 0.03	 4.52 ± 0.03 	10.81 ± 0.03

Tabel 4.4 Fractional improvements, time interval (T) and number of discontinuities (nd), stations are divided by latitude. (A.Nardo, 2011)

Site	F_n	F_e	F_u	T[y]	n_d
MCM4	0.03	-0.02	-0.03	2.2850	0
VESL	-0.06	0.01	-0.08	2.2820	0
SYOG	-0.01	0.00	-0.02	2.2820	0
DAV1	0.03	0.04	-0.02	2.2140	1
MAW1	0.02	0.00	-0.03	2.2710	0
CAS1	0.03	0.12	0.02	2.2850	0
PALM	-0.03	0.01	0.01	2.2820	0
KERG	0.02	-0.01	0.00	2.2850	0
ALIC	0.01	0.20	0.19	2.2850	1
GUAM	0.01	-0.03	0.00	2.2850	1

For the considered stations, VCV matrices have been extracted from the SINEX files and converted to the NEU (North East Up) reference system. As we see the improvement derived from the variance-covariance matrix is approximated with the following relation:

Ellipse of blue and red errors (95%) are the empirical calculations based on single GPS and GPS + GLONASS combined observations, while black and green ellipses are those derived from daily variance-covariance matrices. Figure 4.1.5 illustrates the errors of any errors of any reference network effect.

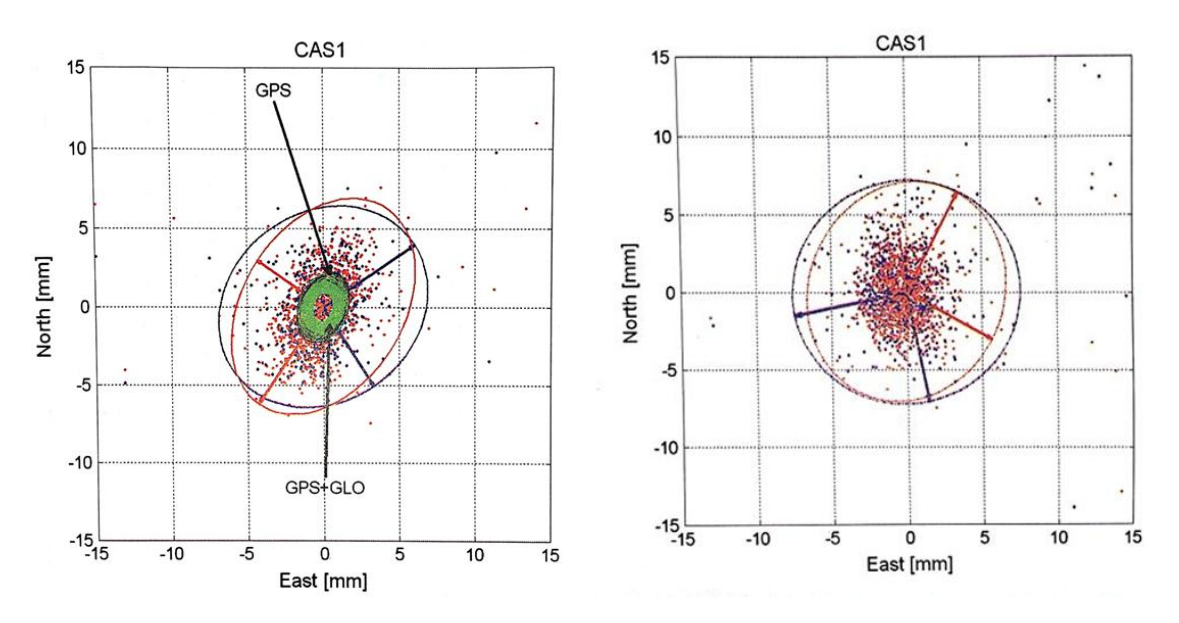


Fig.4.5 – Scatterplot derived in both cases (A. Nardo, 2011)

Discussions and results

In conclusion, this two-and-a-half-year long period of daily analysis was conducted to assess the long-term impact of the GLONASS system on geodynamic studies and reference frame maintenance. In such a case the improvement of the formal accuracy of the coordinates for certain stations of the network was obtained with the help of the following relationship:

$$Q_{GPS+GLONASS} = \frac{\alpha}{1+\alpha} Q_{GPS}$$
 (4.4)

Discussion: α - is the Bruyninx factor (2006) and represents the ratio between the number of GPS satellites and the number of GLONASS satellites.

At the same time, the stability of the reference frame is not affected by the additional GLONASS observations.

The fact that formal errors are mainly in harmony with relations (4.3) and (4.4), while empirical errors are not (as we see in Figure 4.5), could demonstrate a modeling problem.

According to Dach's publication (2011), in the case of GPS observations, Phase Center variation (PCV) may cause a mean difference of up to 1 cm in the modeling of the L3 phase observable for the GLONASS system (when compared to the GLONASS-specific PCVs), which is partially absorbed by the GPS-GLONASS system bias, furthermore, the error of the GLONASS space system orbit should be taken into account because it represents the double error of the corresponding error for the GPS system, causing an error of 4mm on baselines of 2000 km.

There is sufficient room for improvement of the functional and stochastic model, a rough estimate based on the number of observations shows a sub-millimetric improvement of

the combined GPS + GLONASS system. In a near future scenario when the number of GPS satellites will equal the number of GLONASS satellites, the improvement of the precision of the daily estimates of the coordinates will still be around 30%. (A.Nardo, 2011)

4.2. Precise Point Positioning using Single-GPS and GPS + Galileo

With the lauch of the new Galieo satellites, a PPP solution based on the combined GPS/Galileo measurements is feasible. Combining GPS and Galileo systems offers more visible satellites, which is expected to enhance the GDOP and the overall solution (Hofmann-Wellenfof 2008). In order to take full advantage of the new Galileo signals, it is essential to rigorously determine the stochastic characteristics. Galileo observations sessions were used to study the stochastic characteristics of the Galileo E1 signal. As a byproduct, the stochastic characteristics of the P1 signal, are also determined in order to verify the stochastic model developed by the Galileo signals. (Akram Afifi, 2013)

The combined GPS and Galileo L1 / E1 signals were used to check the stochastic model.

To verify the obtained results, the stochastic model is developed in order to evaluate the effect of stochastic characteristics in the GPS / Galileo combined PPP system, precision and convergence time..

The result of the combination of GPS observations and Galileo show a sub-decimeter accuracy and an improvement up to 30% of the convergence time.

GNSS observations are affected by random and systematic errors that need to be taken into account in order to achieve accurate positioning. Precision positioning accuracy depends on the ability to reduce a series of errors. These errors can be classified into three categories: satellite errors, satellite signal propagation errors, and receiver / antenna configuration errors (El-Rabbany, 2006).

In addition to the errors above, additional errors arise due to the combination of the two systems in a Precise Point Positioning (PPP) model such as the GPS To Galileo time offset (GGTO), due to the fact that each system uses a different time frame. The GPS system uses the GPST time system that refers to the UTC as maintained by the US Naval Observatory (USNO). On the other hand, the Galileo space system has its own time frame called The Galileo system.

Moreover, GPS and Galileo measurements are expressed in different reference frames which should be taken into account in the estimation of the combined PPP solution.

The receiver measurement noise results from the electronic limitations of the receptor. Determination of the noise level of GNSS observations can be performed by testing the receivers. Two tests are normally used to determine the noise level of the receiver, namely the zero and ahort baselines tests. The zero baseline test uses an antenna, followed by a signal splitter that serves two or more GPS receivers. Several receiver problems can be examined through the zero baseline test, including interchannel biases and cycle slips.

Using a common antenna cancels systematic errors such as multipath and preamplifier noise. The short baselines test, on the other hand, uses two receivers that are several meters apart on two consecutive days. In this case, double difference residuals ofe one single day would contain the system noise and the multipath effect.

As the multipath effect repeats daily for a GPS system, differencing the double difference residuals of two consecutive days will cancel the multipath effect and the system noise will remain. The multipath effect is not iterative for the Galileo space system, Galileo's orbit parameters lead to a period of about 14 hours, 4 minutes and 45 seconds, and a repeating cycle of the tracked position is 10 days, which is equivalent to 17 cycles. (Hofmann-Wellenhof, 2008)

A short baseline test is used to determine the stochastic characteristics of the Galileo E1 signals. This test is usually performed using the same type of receiver. Unfortunately, two different receivers were available in the test to make Galileo observations. This, however, has been taken into account in data processing. By differening pseudoranges and carrier phase equations corresponding to each receiver, cancel out the geometric term, error due to the non-synchronization of satellite and receiver clocks, and tropospheric delays are canceled. The remaining parameters include satellite and receiver hardware delays, ionospheric error, ambiguity parameter and the system noise.

The phase measurement noise was neglected due to its small size compared to pseudorange measurements (Elsobeiey and El-Rabbany, 2010). The receiver hardware is assumed to be stable during the observation period of approximately four hours in this case, while the ambiguity parameter and the the initial phase bias are constants for a continuous measurement session (Hofmann-Wellenhof, 2008). As such, these parameters can be removed from the model by differencing relative to the respect of the first value of the series. (Akram Afifi, 2013)

The stochastic model properties of the observations are reflected in the observations weight matrix that includes absolute and relative accuracies relative to one another. In the PPP modeling, most of the available observations stochastic models are empirical models, such as the sine or cosine model, the exponential model, and the polynomial models. All these stochastic models are dependent of the satellites elevation angles. These models can not be sufficiently precise for models of all receivers and the new GNSS frequencies.

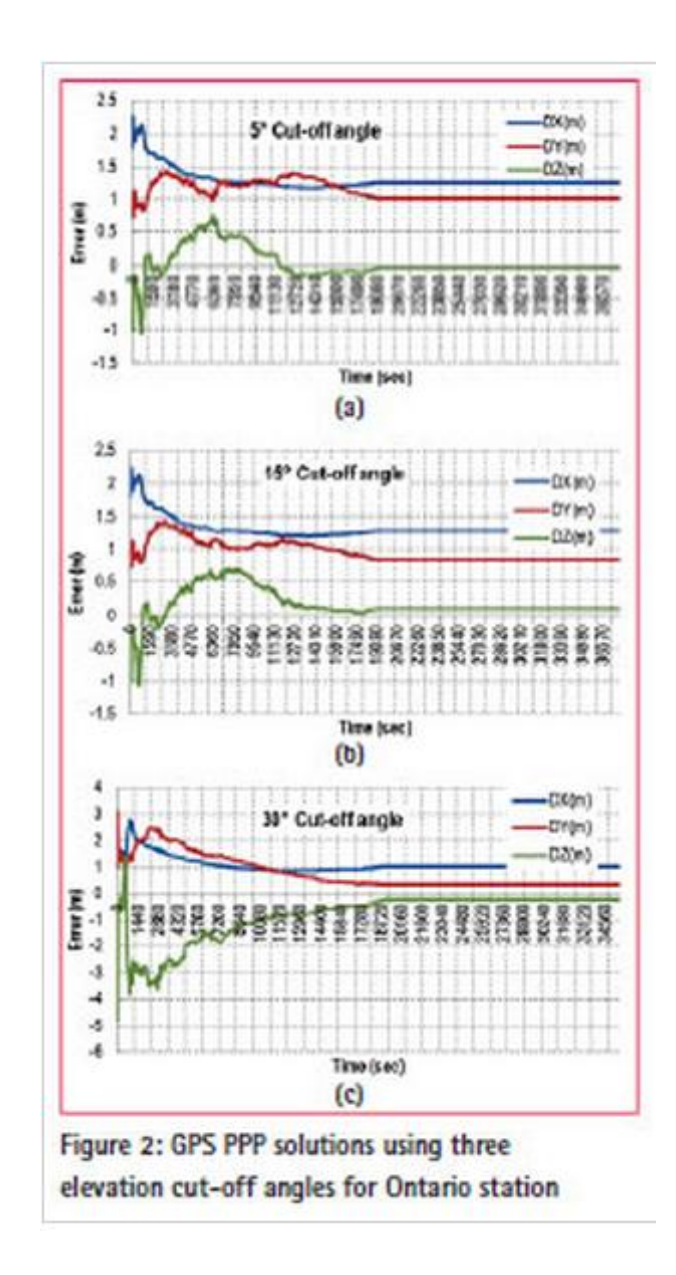


Fig.4.6 - Accurate GPS PPP positioning using three elevation cut-off angles for the Ontario station (Akram Afifi, 2013)

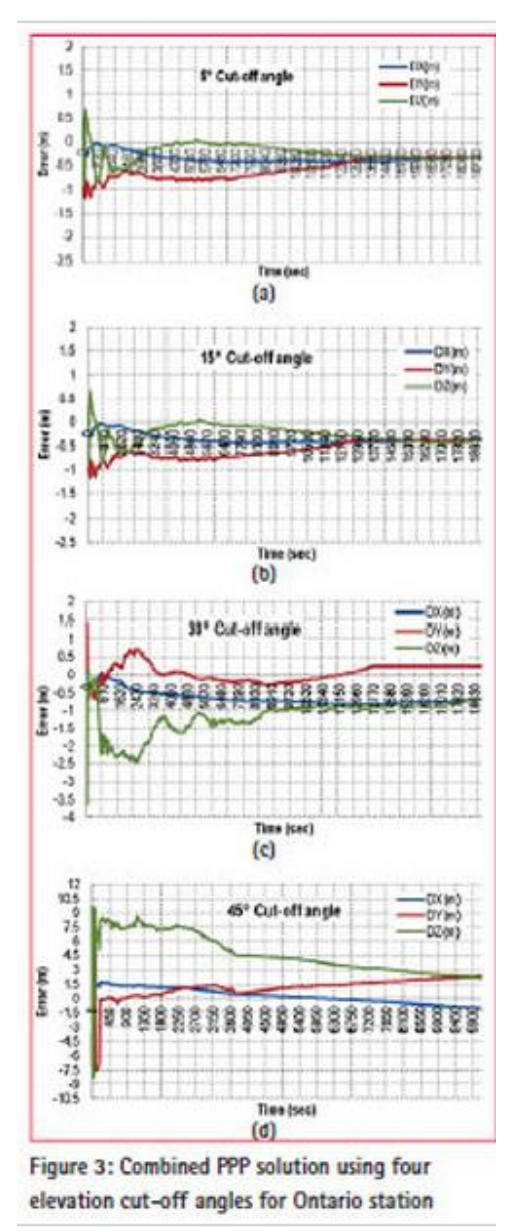


Fig.4.7 - Combined PPP Precise positioning using four elevation cut-off angles for Ontario Station (Akram Afifi, 2013)

The differentiated measurements presented are divided into nine compartments according to the satellite elevation angle, from 0 $^{\circ}$ to 90 $^{\circ}$ with an increment of 10 $^{\circ}$ (0 $^{\circ}$ to 10 $^{\circ}$, 10 $^{\circ}$ to 20 $^{\circ}$, etc.). The least square best-fit model (which provides a prediction of the standard deviations) and satellites elevation angles is used to form the stochastic model.

Discussions and results

This study presents a combined Precise Point Positioning (PPP) solution using the L1 (GPS) and the E1 (Galileo) frequencies.

The GPSPace PPP software from Natural Resources Canada (NRCan) has been modified to manage data from both GPS and Galileo, which allows a combined GPS + Galileo PPP solution. The NOAA ionospheric correction model was used to correct the delay due to ionosphere (Smith, 2004). In addition, the NOAA model is used along the Vienna mapping function to correct the tropospheric delay (Ibrahim and El-Rabbany, 2008). The International GNSS Service provides orbital and lock orrections used by GPS satellites (Kouba, J. 2009). On the other hand, the Giove Cooperative Network for GIOVE Observations (Congo), through its

network, provides information on orbital corrections and Galileo satellite clocks. (MONTENBRUCK et al., 2009).

The PPP analysis is done in two stages: The first step studies the effect of combining GPS and Galileo measurements on the PPP solution in urban environments with a different elevation angle. In the second stage, compares the results obtained from the two stochastic models, the original one and the one developed.

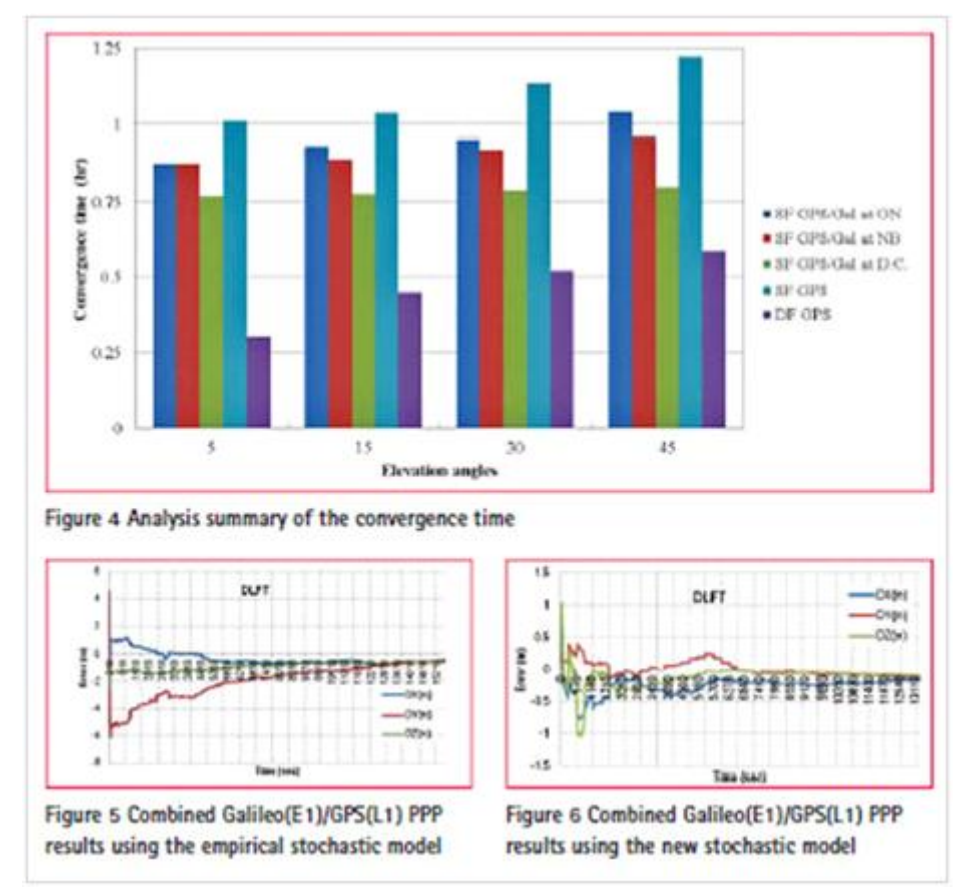


Fig.4.8 - Analysis summary of the convergence time using different stochastic models (Akram Afifi, 2013)

To simulate a densely built urban environment, different scenarios were considered, so different angles of elevation: $5\,^\circ$, $15\,^\circ$, $30\,^\circ$ and $45\,^\circ$ were used in the analysis. In the analysis, GPS + Galileo combined measurements were used at three GNSS stations located in Ontario, New Brunswick and Washington D.C.

Due to space limitation, the results at the Ontario station are presented for both cases: GPS observations and GPS combined observations + Galileo in precise point positioning at different cut-off elevation angles.

Figure **4.6** shows the results of PPP positioning with the GPS system at cut-off elevation angles, namely 5°, 15° and 30°. It is shown that the GPS PPP solution is not possible at an 45° elevation cut-off angle because there are not enough visible satellites.

Figure **4.7** shows the results of the combined GPS + Galieo PPP solution at different cut-off elevation angles, namely 5°, 15°, 30° and 45°. The Galileo system may have more satellites available than the GPS at a 45° cut-off elevation angle for both stations: Ontario and Washington D.C. With the help of Galileo's additional satellites, precise point positioning (PPP) can be performed at a cut-off elevation angle of 45° within the two stations analysed (Ontario and Washington D.C). Figure 4.2.3 points out that decimetric accuracy can be obtained using the single frequency GPS+Galileo PPP in a static application, which is comparable to the GPS dual-frequency solution.

In this case study, it has been demonstrated that the time of convergence in the precise point positioning solution has been improved with the technology of a single frequency GPS + Galileo by 20% to 30% compared to single-frequency GPS solution.

The bottom figures in Figure 4.2.3 show the results of the combination of the two systems using the old stochastic model, respectively the new stochastic model. The results demonstrate that the new model improves both positioning accuracy and convergence time.

In conclusion, the purpose of this study was to combine the Galileo E1 signals with the L1 GPS.

It has been demonstrated that the Galileo satellite system offers more visible satellites at a 45° cut-off elevation angle compared to the GPS system, which makes the PPP solution possible at this high cut-off elevation angle. The results have demonstrated tha a sub-decimetre positioning precision as well as an improvement in the convergence time of up to 30%, possible with the help of single-frequency GPS + Galileo PPP technology. (Akram Afifi, 2013)

4.3. Multi-GNSS RTK Positioning performance in New Zealand

4.3.1. Introduction

The RTK Multi-GNSS technology performance can be reached anywhere on the Globe at any time. The global Satellite constellations includes GPS, Russians GLONASS, Galileo and the BeiDou Navigation Satellite System, whereas the regional constellations are Japanese QZSS and the Indian Regional Navigation Satellite System (IRNSS).

It is analysed the performance of RTK positioning technology with a single initialization base obtained in South Island of New Zealand, a region with a good visibility to GNSS constellations.

Global and regional GNSS systems are expected to reach maximum constellations by 2020. The first results obtained using the BeiDou satellite system (BDS) within precise positioning can be found in Montenbruck 2013. The results of RTK real-time kinematic positioning combining information obtained from these satellite systems have been presented so far in various short and medium-length specialized works. Short baselines are defined when the lengths of the bases are small enough that delays due to the troposphere and the ionosphere can be neglected, but within the long base lengths these delays need to be estimated.

All studies are based on satellite data obtained from GNSS systems in China or Australia. This study presents the performance achieved using Multi-GNSS RTK technology in Dunedin, New Zealand.

The ground tracks of BeiDou, Galileo and QZSS (Apr 29, 2013) as observed from a in Perth, Australia, with an elevation cut-off angle of 10° are shown in Figure 3.3.1. Similar to those obtained on the ground by a receiver located in Duedin are depicted in Figure 4.3.2. The Perth Station tracks 5 GEO, 5 IGSO and 4 MEO BeiDou satellites, 3 Galileo IOV MEO satellites, and a 1 HEO QZSS satellite. (Robert Odolinski, IGNSS 2015)

The Dunedin station records fewer satellites over the day, so the positioning of the Multi-GNSS RTK on a single baseline is expected to be reduced in Dunedin as compared to Perth when combining these satellite systems with the GPS system.

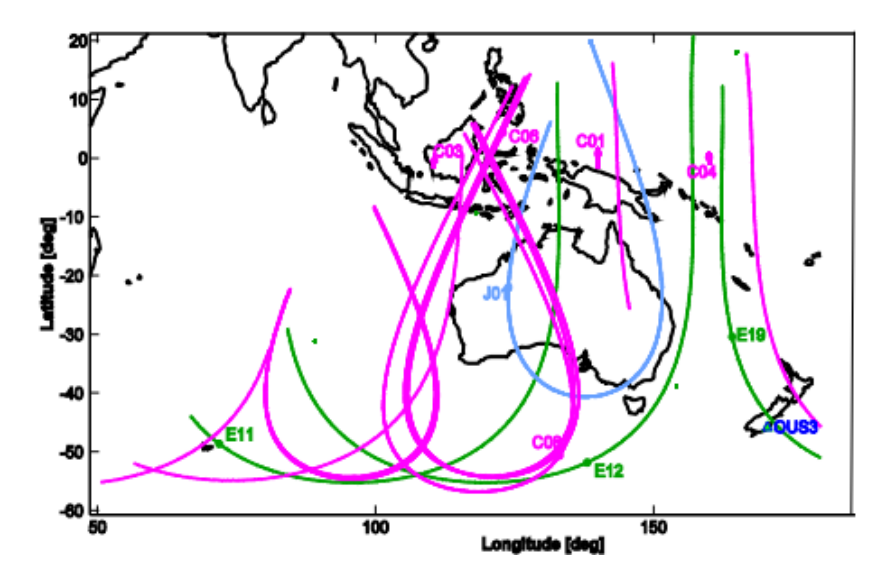


Fig.4.9. Perth recorded satellites (Robert Odolinski, IGNSS 2015)

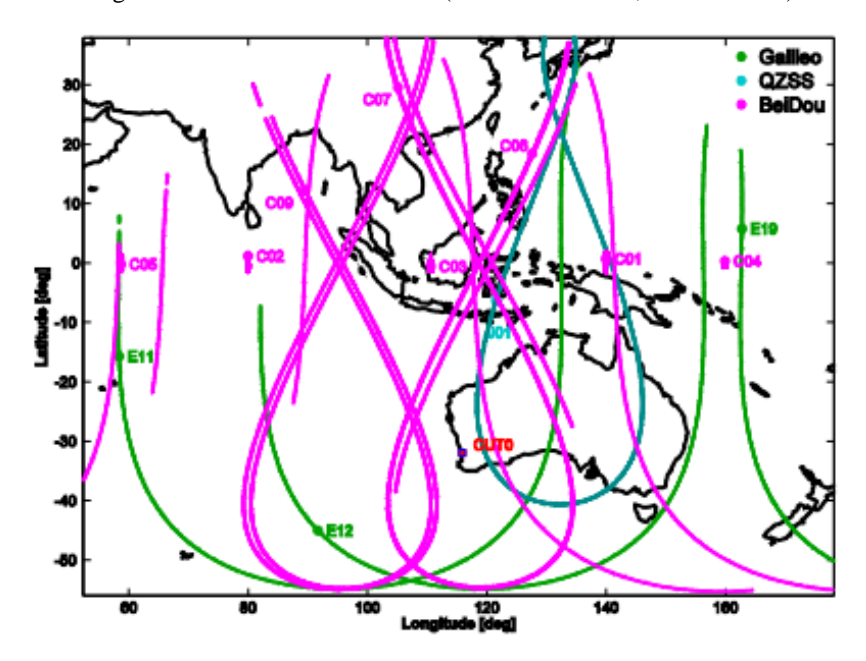


Fig. 4.10. Dunedin recorded satellites (Robert Odolinski, IGNSS 2015)

At the time of the case study, four Galileo satellites were launched in the Full Operational Capability (FOC) phase with the appropriate signals expected to be available for civilian users throughout 2015, as well as the sixth IGSO BeiDou satellite with a B1 frequency centered at the L1 / L1 GPS frequency and at the E1/Galileo frequency. At the time of the case study, they were not available.

Indian IRNSS satellites are not visible in New Zealand, and the Russian Glonass have a single satellite based on Code Division Multiple Access that records a signal that does not overlap with other frequencies used in this case study.

In this case study, the Multi-GNSS RTK is covered on short baselines. The frequenciesthat will be analysed are L1 / GPS, E1 / Galileo, L1 / QZSS and B1 / BeiDou so as to maximize the number of visible satellites with overlapping frequencies. E1 frequency and L1 GPS / QZSS overlap. Future BeiDou satellites will contain the B1 frequency that will overlap the other frequencies in order to create a rigorous functional model combining these four satellite systems. (Robert Odolinski, IGNSS 2015)

4.3.2. Multi-GNSS single-baselines functional models

The RTK model obtained from observations from the four GNSS systems is presented in Odolinski (2015 a) and is based on between-receiver single-differenced (SD) observations. The model is based on the S-system. The single-differenced (SD) model eliminates satellite-dependent parameters, thus eliminating satellite clock error, satellite hardware code, and initial phase delays, also eliminating orbital errors as well as errors due to signal propagation satellite through the atmosphere (due to short baselines). Within this model the inter-system bias is estimated.

Consider r = 1,2 receivers tracking the GPS satellites and GNSS systems satellites marked with $s_G = 1_{G,...,m}m_G$ and GNSS satellites marked with * s*=1*,...,m*, where * represents either Galileo (E) satellites or QZSS (Q) or BeiDou (B) respectively. The linearized full-rank SD system of observation equations considering overlapping frequencies j = 1, ..., f then reads (in units of range):

$$p_{12,j}^{S_G} = -c_2^{S_G^T} \Delta x_{12} + \widehat{dt_{12}} + \widehat{dt_{12}}_{j}$$

$$\phi_{12,j}^{S_G} = -c_2^{S_G^T} \Delta x_{12} + \widehat{dt_{12}} + \widehat{\delta_{12,j}^G} + \lambda_j \hat{z}_{12,j}^{1_{GS_G}}$$

$$p_{12,j}^{S_*} = -c_2^{S_*^T} \Delta x_{12} + \widehat{dt_{12}} + \widehat{dt_{12}}_{j} + \widehat{dt_{12}}_{j}^{G_*}$$

$$\phi_{12,j}^{S_*} = -c_2^{S_*^T} \Delta x_{12} + \widehat{dt_{12}} + \widehat{dt_{12}}_{j} + \widehat{dt_{12}}_{j}^{G_*} + \lambda_j \hat{z}_{12,j}^{1_{*S_{G^*}}}$$

$$(4.5)$$

Where $(.)_{12} = (.)_{2}$ - $(.)_{1}$ is the difference between-receiver SDs notation, $p_{12,j}^{s}$ and $\Phi_{12,j}^{s}$ represents the code and phase observables respectively, $c_{r}^{sT} = (x^{s} - x_{r})^{T} / \|(x^{s} - x_{r})\|$ is the line-of-sight unit vector from the receiver r to GNSS satellites s obtained by linearizing the system of equations depending on the receiver's coordinates.

Estimation of unknowns:

 $\Delta x_{12} = \Delta x_2 - \Delta x_1$ – the relative receiver coordinates,

 $d\widetilde{t_{12}} = dt_{12} + d_{12}^G$ - relative receiver clock with GPS differential code delay,

 $\tilde{d}_{12}^G=d_{12,j}^G-d_{12,1}^G$ – relative GPS Differential Code Bias (DCB) estimated for j>1

 $\tilde{d}_{12}^G=\delta_{12,j}^G-d_{12,1}^G+\lambda_jz_{12,j}^{1.G}$ – relative GPS receiver hardware (HW) phase delay

 $\tilde{d}_{12}^{G*}=d_{12,j}^*-d_{12,j}^G$ – differential code ISB

 $\tilde{\delta}_{12,j}^{G*}=\delta_{12,j}^*-\delta_{12,j}^G+\lambda_jz_{12,j}^{1\,G1*}$ – differential phase ISB biased by a DD inter-system ambiguity

$$\tilde{z}_{12,i}^{1_G s_G} = z_{12,i}^{s_G} - z_{12,i}^{1_G} - \text{DD GPS}$$
 integer ambiguity

$$\tilde{z}_{12,j}^{1_*S_*} = z_{12,j}^{S_*} - z_{12,j}^{1_*}$$
 - DD BDS, Galileo or QZSS integer ambiguity.

The ambiguities are of integer type following double differentiation, neglecting the phase delays due to the receiver and satellite hardware (HW).

The number of observations, receivers used and satellites used in the case study is shown in the table below:

Table 4.5 A single measurement period, redundancy on a single RTK basis. (Robert Odolinski, IGNSS 2015)

Model	# of observations	# of unknowns	Redundancy	Solvability condition
Single-system	2f*m*	$3+f_*+f_*m_*$	f*(m*-1)-3	$m* \ge 4$
4-system ISBs-float (1)	$2fm_G+2fm_B+$ $+2fm_E+2fm_Q$	$3+f+fm_G+f+fm_B$ $+f+fm_E+f+fm_Q$	$f(m_G-1)+f(m_B-1)$ + $f(m_E-1)+f(m_Q-1)-3$	$m_G + m_B + m_E + m_Q \ge 7$
4-system, ISBs-fixed assuming all frequencies overlap (2)	$2fm_G + 2fm_B + + 2fm_E + 2fm_Q$	$3+f+fm_G+fm_B +fm_E+fm_Q$	$f(m_G-1)+fm_B + fm_E+fm_Q-3$	$m_G + m_B + m_E + m_Q \ge 4$
4-system, ISBs-fixed for the overlapping frequencies used herein	$2fm_G + 2f_B m_B + + 2fm_E + 2fm_Q$	$3+f+fm_G+f_B+f_Bm_B$ $+fm_E+fm_Q$	$f(m_G-1)+f_B(m_B-1) + fm_E+fm_Q-3$	$m_G + m_B + m_E + m_Q \ge 5$

4.3.3. Multi-GNSS receiver used in the case study in New Zealand and Australia

This subchapter analyses the system performance of the four RTK models presented in the relationship (4.5) used in the satellite observations over two days in Perth (2013) and Dunedin (2015). Comparisons will be made with the use of single-GNSS or multi-GNSS techniques.

Data collection. The zero baseline used for the inter-system byas (ISB) calibration is shown in the figure below. Equivalents (3.3.2.1) will be considered as fixed receivers. The zero baseline consists of two receivers connected to the same antenna as to eliminate any multipath effect (satellite signal reflection). If the estimated inter-system byas (ISBs) are time constants, they can be used as a-priori corrections on independent baselines wich collect data one month away in Perth (CUT1-CUTT) and even two years later in Dunedin to maximize the redundancy of the RTK models. The baselines used are up to 1 kilometer in length, neglecting the effects due to the atmosphere. The stochastic models used in the case study are based on Euler and Goad (1991) exponential elevation weighting functions, as well as Zenith-referenced a priori codes and phase standard deviations (STDs) in undifferentiated observations. Standard deviations are shown within brackets.



Fig.4.11. Zero-Baseline Receiver used in Perth (2013-2014) for inter-system by as calibration (Robert Odolinski, IGNSS 2015)



Fig. 4.12. Dunedin receiver used in the multi-GNSS RTK performance analysis (Robert Odolinski, IGNSS 2015)

Table 4.6. Zenith-referenced code-phase a priori standard deviations determined in the Dunedin multi-GNSS performance analysis (standard deviation determinations in Perth are shown within brackets). (Robert Odolinski, IGNSS 2015)

Sat. system	Frequency	Code [cm]	Phase [mm]
GPS	L1	25 (30)	2(2)
BDS	B1	30 (35)	2(2)
Galileo	E1	30 (30)	2(2)
QZSS	L1	30 (30)	3 (3)

4.3.4. Results

The total number of satellites tracked by Perth receivers over one day data in 2013, respectively visible in Dunedin in 2015, is shown in Fig. 4.3.4.1. at an elevation cut-off angle of 10°.

Although one of the Galileo IOV satellite was not received in Dunedin, we can see a considerably larger number of satellites registered by the Dunedin receivers. However, due to the high visibility of the Asia Pacific region, the number of recorded satellites is higher over a day compared to Dunedin.

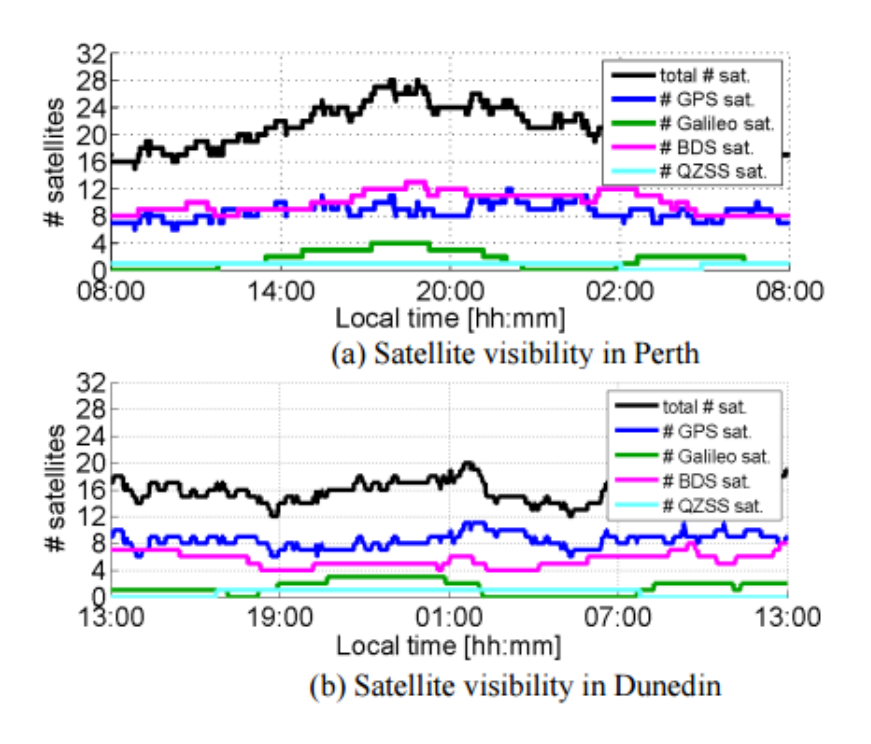


Fig. 4.13 Visibility of satellites in Perth and Dunedin over a day (Robert Odolinski, IGNSS 2015)

The LAMBDA method is used for ambiguity resolution (Teunissen 1995), and the detection, identification and adaption (DIA) is performed in order to eliminate outliers (Teunissen 1990).

The daily average of estimated inter-system byas in Perth using the zero-baseline setup was shown to be useful over two separate days by one year (2013 vs 2014). Inter-system corrections applied to receiver pairs in Perth (2013) can be applied to receiver pairs in Dunedin (2015). Recent studies have shown that the multi-GNSS between-receiver differential code biases (DCBs) may vary over one year interval.

The Success Rate was determined based on the variance-covariance matrix corresponding to float ambiguities wich is a precise lower bound to the least squares method (ILS). Since it is a formal measure, it can be used a-priori any GNSS measurements are collected and to be a prediction indicator in determining whether ambiguity resolution is expected to be successful.

The rate of success (single-epoch bootstrapped SR) measured over a measurement period for elevation cut-off angles ranging between 10° -35° is shown in the figure below, based on satellite observations over two days of 2013 in Perth, respectively based on satellite observations in Dunedin (2015) (Febr 6-7, 2015) at bottom. The RTK kinematic positioning method using L1 GPS only is shown in blue, ie L1 + E1 GPS + GALILEO with green, E1+L1+L1 Galileo+GPS+QZSS with red and B1+L1 Beidou+GPS with cyan and a four-system multi-GNSS based on the four GNSS systems - B1 + E1 + L1 + L1 Beidou + Galileo + GPS + QZSS is displayed in black. Dotted lines are the float models (ISBs-float) used in inter-system ISB determination. Models represented by red dotted or black dotted lines are models of double or triple system model equations. The QZSS satellite can not contribute to modeling as required in estimating inter-system bias.

Since fewer GPS satellites and a Galileo IOV type satellite are tracked in Dunedin compared to the number of satellites tracked in Perth, the figure below shows the success rate using an $\rm E1+L1+L1$ Galileo + QZSS + GPS RTK model displayed as a green line in Perth at top of figure. (Robert Odolinski, IGNSS 2015)

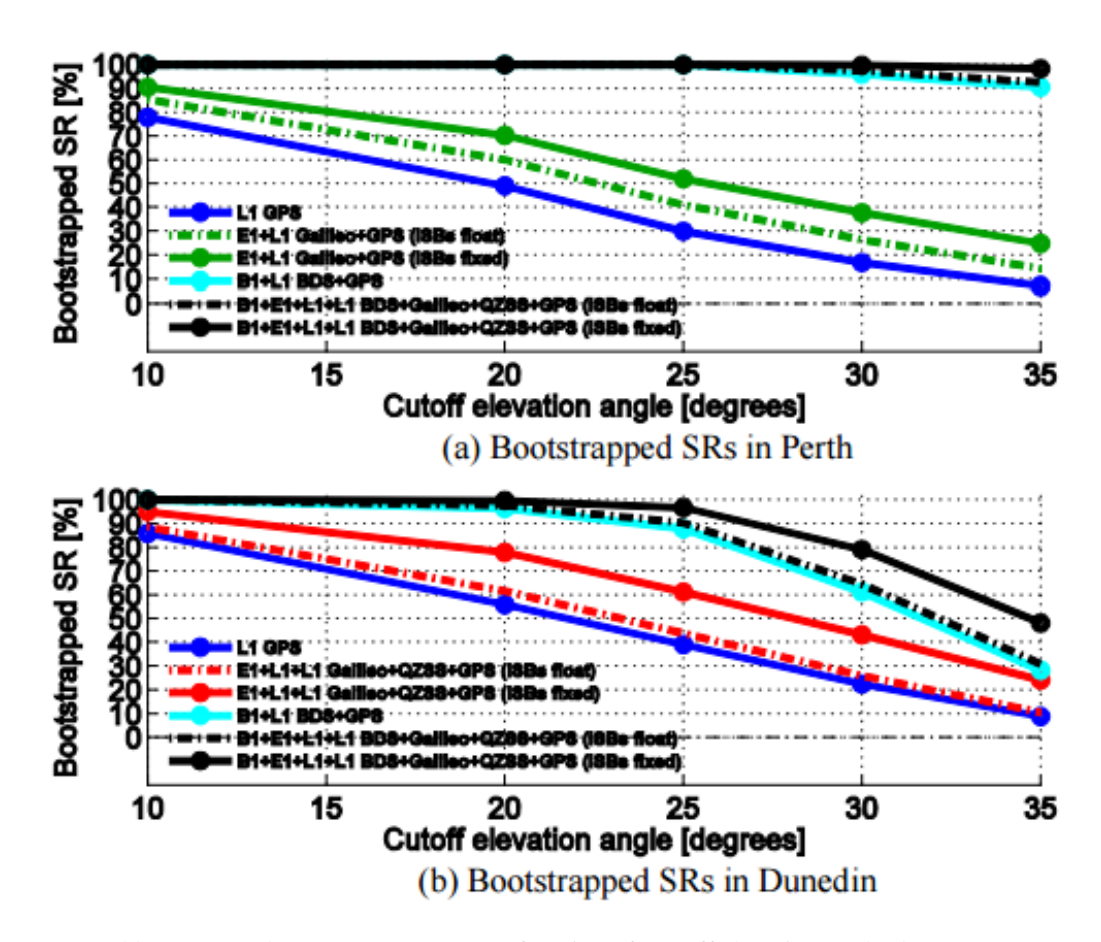


Fig. 4.14. Formal bootstrapped success rate (SR) as a function of cut-off elevation angles between 10° to 35°. The bootstrapped success rate (SRs) are taken as a mean over April 29-30, 2013 in Perth (a) and February 6-7, 2015 for Dunedin (Robert Odolinski, IGNSS 2015)

The L1 GPS success rate in Dunedin is high for all cut-off elevation angles, which leads to better GPS code positioning accuracy for two receivers in Dunedin. The Galileo + GPS ISBs float model in Perth resembles the E1 + L1 + L1 Galileo + GPS + QZSS ISBs-float model SRSs in Dunedin for all cut-off elevation angles. The success rate increases when inter-system bias ISBs are fixed for both models, especially for observations made in Dunedin.

The additional Galileo and QZSS observations improve positioning accuracy when the number of visible satellites is low, therefore inter-system calibration is very important in low-visibility satellite environments. The success rate increases substantially with the addition of BeiDou observations to GPS observations, in this case the success rate reaches a 100% threshold in Perth for cut-off angles of up to 25° and for models corresponding to the four systems.

The corresponding elevation angles in Dunedin are in the 10°, 20° range when inter-system errors are determined (full black lines). The performances differences with respect to Perth is mainly due to the lower number of BeiDou satellites tracked in Dunedin. By comparing the four-System success rate (SR) of 100% to a single GPS system SRs, for elevation angles of approximately 20°, the SR indicators have a value close to 50% for both locations. (Robert Odolinski, IGNSS 2015)

An empirical analysis of the performance of multi-GNSS RTK technology on single baseline

Real data was used to demonstrate the current performance of the four-system RTK models. The empirical integer least squares (ILS) success rates (SR) is computed by comparing the

determined integer ambiguities in a single epoch to a reference set. The reference ambiguities were determined by using a four-system multy-frequency RTK model with fixed receiver positions, the Kalman filter, and a dynamic model in which ambiguities are treated as time constant over the two-day observation period.

The number of correctly fixed epochs divided by the total number of positioning epochs provides the SR type indicators of the ILS method. The ILS SRs indicators determined within a single measurement period are shown in the Table 4-7 for different system combinations as can be seen in the Figure for both locations of interest, where the 100% SR indicator values are shown in bold.

The inter-system bias (ISB) model is marked with "a", and the model in which inter-system biases (ISB) are ignored is displayed with "b". The pattern in which inter-system errors are ignored is the same as that set in Equation (4-5) except code / phase corrections specific to inter-system errors are incorrectly equal to zero for GNSS mixer receivers. Ignoring the inter-system biases leads to a decrease in the success rate (SR) shown in the table at b. The float inter-system correction model is shown in letter c and provides an image of the SR type indicators, being lower than the established one.

The table based on real data verified the predictions in Figure 4.14, since almost all ILS SRs-type indicators are larger than the corresponding bootstrapped SRs. For 10° cut-off elevation angles, this prediction does not apply because in both locations (Perth and Dunedin) the multipath effect at this elevation angle has been felt for a growing number of GPS satellites and the BeiDou GEO C03 satellite. Finally, the table illustrates that combining satellite systems at elevation angles of more than 10° is feasible if one of the systems can achieve continuously ambiguity resolution at these angles.

Table: 4-7 Empirical ILS SR Indicators in the case of single-frequency RTK positioning and cut-off elevation angles considered in the range 10° -35°. The bootstrapped success rate (SRs) are computed based on April 29-30, 2013 for Perth and over February 6-7, 2015 for Dunedin. A=ISBs fixed model, b = ISBs-ignored and c=ISBs-float model (Robert Odolinski, IGNSS 2015)

Location and system/frequency	ISBs	Empirical ILS SR [%]				
cutoff [°]:		10	20	25	30	35
Perth						
GPS L1	-	84.5	60.9	40.3	24.5	11.0
E1+L1 Galileo+GPS	a	92.7	78.2	60.8	46.2	31.4
	b	37.4	29.9	20.7	12.9	5.7
	c	88.9	70.3	50.8	35.5	20.3
B1+L1 BDS+GPS	-	98.4	100	100	96.8	91.9
B1+E1+L1+L1	a	98.4	100	100	99.8	98.7
BDS+Galileo+QZSS+GPS						
	b	97.7	93.6	88.8	78.9	71.3
	c	98.4	100	100	97.7	93.3
Dunedin						
GPS L1	-	90.1	57.7	40.5	23.7	9.8
E1+L1+L1 Galileo+QZSS+GPS	a	96.6	79.3	62.2	42.8	23.5
	b	62.1	37.4	25.6	14.3	6.8
	c	92.6	64.5	46.2	28.0	13.1
B1+L1 BDS+GPS	-	97.9	97.8	88.9	64.2	28.2
B1+E1+L1+L1	a	97.9	100	97.2	80.9	48.5
BDS+Galileo+QZSS+GPS						
	b	85.2	76.8	67.0	46.8	22.7
	c	97.9	98.7	91.9	67.7	31.6

Positioning when inter-system biases (ISBs) are ignored and fixed respectively.

Inter-system biases have a major effect in determining the RTK multi-GNSS positioning performance. Empirically, the table shows the effects of these errors in determining the SR indicators.

Figure 4.15 shows RTK positioning results for L1 GPS (left) E1+L1 Galileo+GPS if inter-system biases are ignored or fixed, respectively, fon an elevation cut-off angle of 10° in Perth over two days of data (2013). The a-priori inter-system biases corrections were determined based on the independent zero-baseline set one month before being extracted and considered to be constant values based on the code / phase observations equations respectively. Corrected fixed positions are displayed in green, incorrectly fixed in red, and float solutions in grey for the horizontal and vertical scatter (top two rows). With a light green colour, the number of Galileo satellites are displayed to demonstrate the redundancy difference to the single-GPS model as well s the relation between incorrectly fixed solutions and when ISBs are ignored.

Figure 4.15 illustrates that the correctly fixed solutions are of a two-fold order at the mm-cm level when compared to the non-fixed or float solutions at the dm-m order. At the same time, all measurement epochs are incorrectly fixed ISBs are neglected for the GALILEO + GPS model E1 + L1 (when Galileo satellites are available). The ILS success rate (SR) is 37.4%. Combining the Galileo observations with the GPS, provides ILS SRs when compared to a single GPS system, after correcting the inter-system biases (92.7% vs. 84.5% ILS SR), due to the increase in the number of available satellites.

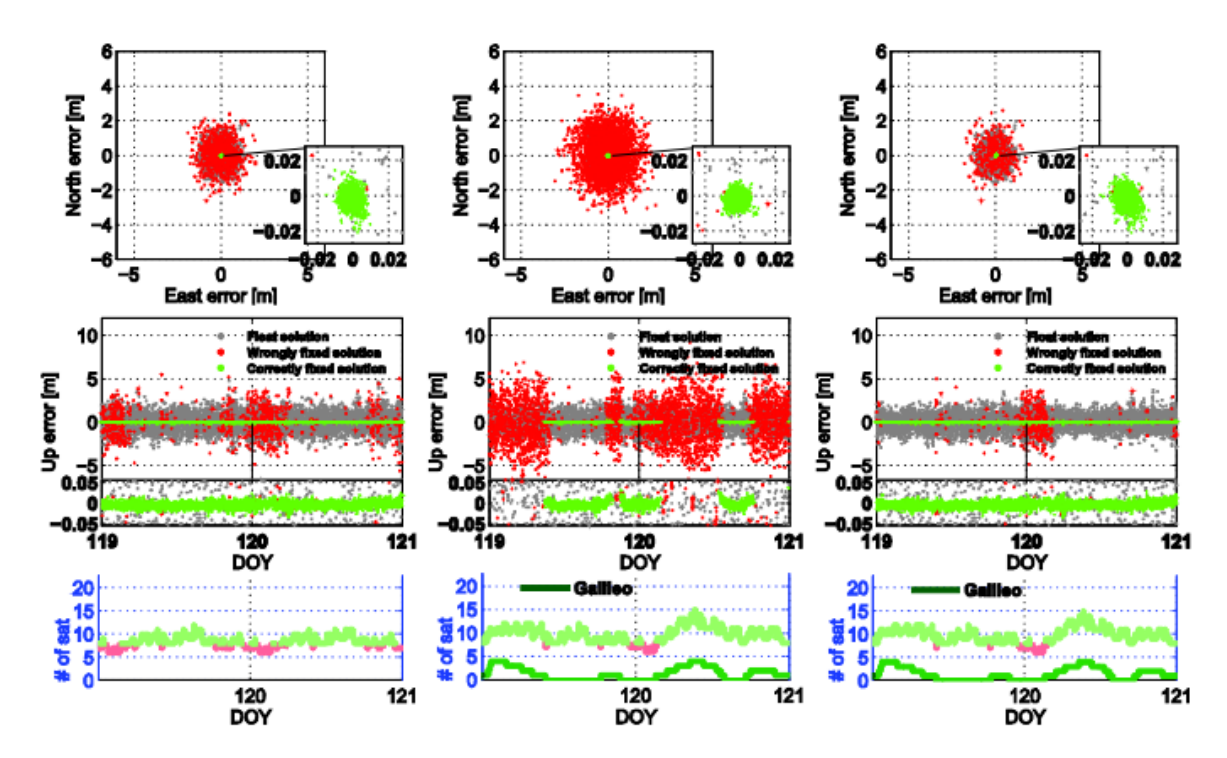


Fig.4.15. L1 GPS (left column) with an ILS success rate of 84.5%, ILS SR E1 + L1 Galileo + GPS ISBs ignored (middle column) with a SR indicator of 37.4%; E1 + L1 GALILEO + GPS (right column) if the intersystem errors are determined with a SR indicator of 92.7% for a single measurement epoch in Perth (2013). The float (gray), incorrectly-fixed (red) and correctly-fixed (green) solutions are given in local North, Eat, Up errors and for a cut-off angle of 10°. The total number of satellites are shown in light green (in red when below eight and Galileo satellites is given in dark green). (Robert Odolinski, IGNSS 2015)

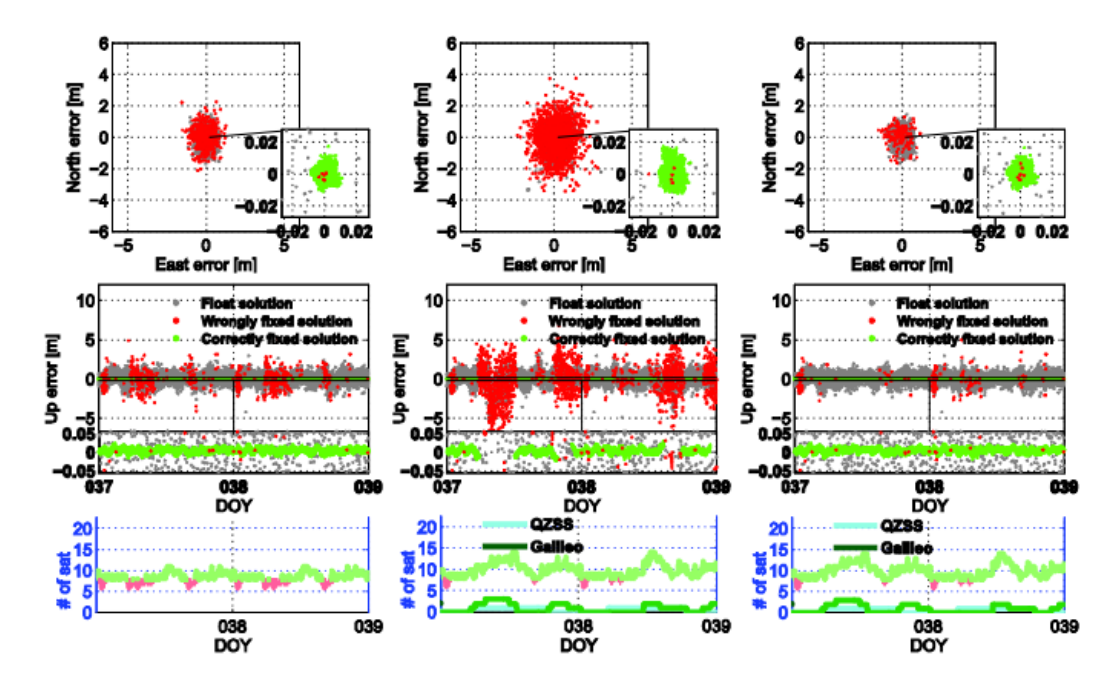


Fig. 4.16. . L1 GPS (left column) with an ILS success rate of 90.1%, E1 + L1+L1 Galileo + GPS + QZSS (middle column) if inter-system biases are ignored with a SR indicator of 62.1%; E1 + L1 + L1 + GALILEO+GPS+QZSS (right column) if inter-system biases are determined with a SR indicator of 96.6%. The results are displayed for a single measurement epoch in Dunedin (2015). The float (gray), incorrectly-fixed (red) and correctly-fixed (green) solutions are given in local North, Eat, Up errors and for a cut-off angle of 10°. The Galileo/QZSS satellites are shown in dark green and cyan respectively. (Robert Odolinski, IGNSS 2015)

Positioning at higher cut-off elevation angles.

Positioning at cut-off elevation angles greater than 25° (and up to 30°) in Perth made it possible to perform continuous RTK positioning over two days. This was provided by combining BeiDou and GPS systems or combining the four systems. The corresponding elevation angle in Dunedin was 20° .

It is of interest to see what happens to the RTK technique performance when the elevation cut-off angles are higher. Figure 4.17 shows the results of instantaneous RTK positioning for an elevation cut-off angle of 25 $^{\circ}$ in Dunedin over two days (2015). On the left is shown the L1 GPS -single model, in the middle column is shown the L1+B1 GPS + BeiDou combined model, and on the right column is shown the model including the four systems with fixed inter-system biases. At bottom of the results, are depicted the PDOP factors for GPS and BDS + GPS to show the relationship between large excursions in the positioning errors and when the satellite-receiver geometry is poor. The system comprising four different satellite constellations does not suffer if the PDOP factors are high.

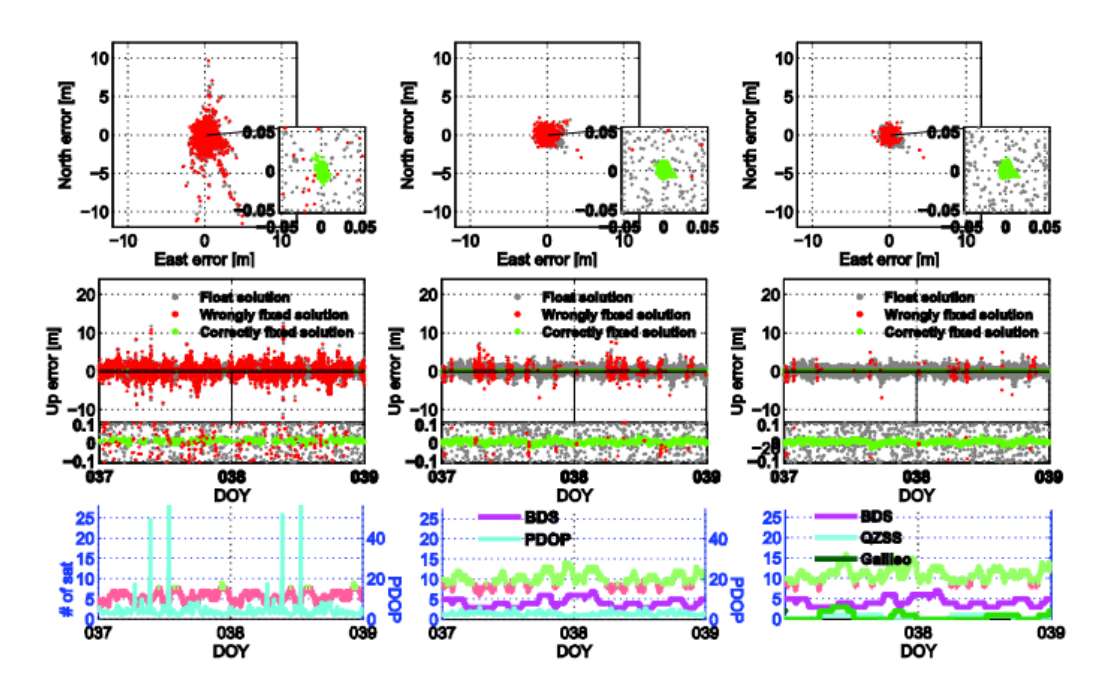


Fig. 4.17. SR indicators in the case of inter-system biases -fixed, respectively ignoring these errors for different satellite configurations: L1 GPS (left column) with a success rate of 40.5%, B1 + L1 BDS+GPS (in the middle) with a SR indicator of 88.9%, B1+E1+L1+L1 BDS + GALILEO + GPS + QZSS (right) with a SR indicator of 97.2% corresponding to ILS SR (right column). The RTK positioning results are for Dunedin (February 6-7, 2015). The float (gray), incorrectly-fixed (red) and correctly-fixed (green) solutions are given for a 25° cut-off angle. The number of satellites are shown in light green (in red when below 8 and 9 when BDS is included, dark green is Galileo and cyan the single QZSS satellite). PDOPs (in cyan) are given for GPS and GPS + BDS (Robert Odolinski, IGNSS 2015)

Figure 4.17 highlights the disadvantages of using a single GNSS system in RTK positioning at higher cut-off elevation angles. The number of satellites is not enough to provide a positioning solution along a two-day session (the L1 GPS case with a 97.3% availability in positioning). The ILS SR indicators for the single-GPS system are only 40.5% and some positioning solutions suffer due to poor satellite-receiver geometry as given by very large PDOP values. By adding BeiDou observations, 100% availability is increased in the positioning, and the ILS SRs indicator for a combined BDS + GPS system achieves 88.9%, and using a combined system of four satellite systems, SR indicators achieves a value of 97.2%. (Robert Odolinski, IGNSS 2015)

5. CONCLUSIONS

This research report analysed the results of various research organizations involving teachers, scientists, engineers on the use of multi-GNSS technology in different situations. At the same time, information on the MGEX (Multi-GNSS Experiment) program within IGS was analysed, analysing all GNSS satellites signals. The Analysis Center provides a characterization of satellites, new signals received, and the ability to develop new software capable of processing data from multi-GNSS systems.

At the same time, the results obtained in case studies on stochastic indicators, the degree to which the reflection phenomenon of the satellite signal is eliminated, the functionality of the method in areas where the visibility is reduced (densely built environments, covered with vegetation, mountainous areas), the degree to which a single GNSS system can be used in these environments and the specific positioning accuracy.

It was also analised the positioning methods used in various case studies, the extent to which additional observations help to improve positioning accuracy, the order of accuracy magnitude obtained in both cases (single-GNSS, multi-GNSS), and last but not least the need to implement a Galileo European satellite positioning system to achieve a viable solution.

To date, the results of various researchers have shown a low degree of improvement in the Glonass observations of the US NAVSTAR-GPS system. The Galileo European system expects to significantly improve positioning accuracy, so it is studied the extent to which additional observations increase the viability of this system by using a combined positioning solution.

It was presented the algorithm used by Professor Teunissen whereby each daily session of measurements was processed in parallel using the strategy illustrated in **Figure 4.1.2.b**. The strategy involves four steps: (1) Data Preparation (data download, reformatting of the files), (2) Data editing (synchronization of receivers clocks, cycle slip detection, estimation of a first approximation solution), (3) Ambiguity Resolution (4) Final adjustment.

The GPS IGS and the GLONASS (IGL) were merged into one file (box MERGE), and the scheduling of the receiver's clock was performed using GPS codes. For each daily session of satellite observations, bases have been defined to maximize GPS observations.

A float double differenced solution, based on the ionosphere free model, was obtained by processing a group of five individual stations and combining the normal group equations to determine an approximate solution of the network. The ambiguities are fixed by integer values based on the Quasi Ionosphere Free model. Each base is processed separately, keeping fixed the ZTDs and the coordinates of a single station estimated in the float solution.

No attempt has been made to estimate GLONASS ambiguities, as the ambiguity resolution strategy used can be applied only for bases not exceeding 20 km.

The high number of satellite observations due to the inclusion of GLONASS observations should have a contribution in estimating station coordinates as well as in ZTDs determination, but this improvement is reduced by an increase of the number of parameters to be estimated, mainly the GLONASS float ambiguities.

Taking into account long-term processing, coordinate estimates are taken into account by two daily processings (GPS and GPS + GLONASS) in order to evaluate the possible accuracy improvement (i.e. the standard deviations of the coordinates). The results are reported for stations located in Antarctica (seven stations in total), Australia and the other 2 stations located

on the edge of the APREF network, in order to emphasize the possible effect of the better observation geometry due to GLONASS orbit inclination at high latitudes.

In conclusion, this two-and-a-half-year period of daily analysis was conducted to assess the long-term impact of the GLONASS system on geodynamic studies and reference frame maintenance. From 2009 to April 2011, there was an improvement in the positioning accuracy of the permanent stations using the Glonass observations. Due to the fact that the Glonass Russian positioning system was not fully functional at that time, reaching the 24 satellites constellation on 3 orbital planes in December 2011, it was concluded that the improvement in positioning accuracy is 30%.

Although the Glonass system constellation was not fully operational with a smaller number of satellites (a mean of 2-3 satellites), the Glonass observations helped improve positioning accuracy based on improved satellite geometry. These improvements are important in cinematic applications, in obstructed areas of low visibility vegetation, in densely built areas, canyons, mountainous areas.

With the lauch of the new Galieo satellites, a PPP solution based on the combined GPS/Galileo measurements is feasible. Combining GPS and Galileo systems offers more visible satellites, which is expected to enhance the GDOP and the overall solution (Hofmann-Wellenfof 2008). In order to take full advantage of the new Galileo signals, it is essential to rigorously determine the stochastic characteristics. Galileo observations sessions were used to study the stochastic characteristics of the Galileo E1 signal. As a byproduct, the stochastic characteristics of the P1 signal, are also determined in order to verify the stochastic model developed by the Galileo signals. (Akram Afifi, 2013)

The PPP analysis is done in two stages: The first step studies the effect of combining GPS and Galileo measurements on the PPP solution in urban environments with a different elevation angle. In the second stage, compares the results obtained from the two stochastic models, the original one and the one developed.

In this case study, it has been demonstrated that the time of convergence in the precise point positioning solution has been improved with the technology of a single frequency GPS + Galileo by 20% to 30% compared to single-frequency GPS solution.

Analysing these two case studies, one can conclude that a technology that would combine all three systems would be viable even in difficult environments, and positioning accuracy is higher compared to single-GNSS technology.

In a study of New Zealand's Multi-GNSS RTK performance, it was analysed both the performance of single-GNSS RTK technology and the multi-GNSS RTK, combining GPS observations with BeiDou, Galileo and QZSS in Dunedin, New Zealand, observations made over two days during 2015, as well as in Perth, Australia (2013).

In both locations, the baselines lengths were considered less than 1 kilometre in order to neglect the atmospheric deays. The overlapping frequencies of E1 Galileo-specific, L1 GPS, L1 QZSS and B1 BDS and using capable mixed-receivers types of recording these combined signals, positioning accuracy is considerably improved. The empirical least squares method used in this case study, which estimates the Success Rate (SRs) indicators, is truly successful when inter-system biases are considered, otherwise the multi-GNSS RTK positioning performance is low not taking into account the influence of inter-system biases. At the same time, if these a priori corrections are taken into account, the SR indicators were much better than if the inter-system errors (ISBs) were ignored / floated.

At the same time it was concluded that the GPS-only RTK positioning solution were affected by the poor receiver-satellite geometry at the 25° elevation cut-off angle, whereas when using a combined system of 4 satellite systems, the positioning performance is greatly improved.

It was concluded that tghe four-system ISBs-fixed RTK technology performenace in Perth and for an elevation cut-off angle of 35° is comparable to the corresponding performance in Dunedin for an elevation cut-off angle of 25° , and the difference in performance for higher cut-off elevation angles between the two sites cand be attributed to the fewer BeiDou satellites that were tracked in Dunedin.

The most important issue emerging from the analysis of this case study is that the SR (Success Rate) determined in Dunedin rises from 57.7% for a GPS-only positioning to 100% for a multi-GNSS positioning including four satellite systems with ISBs-fixed model and a cut-off elevation angle of 20° .

Bibliography

Altamimi Z, Collilieux X, Legrande J (2007): *ITRF2005A new release of the International Terrestrial Reference Frame based on time series of station positions and Earth orientation parameters*. J Geophys Res 112

Amiri-Simkooei AR (2009): Noise in multivariate GPS position time series. J Geodes 83:175-187

A.Nardo, L. a. (2011): Earth on the Edge: Science for a Sustainable Planet. International Association of Geodesy Symposia (pp. 239-246). Melbourne, Australia: Springer.

Akram Afifi, A. E.-R. (2013): Single frequency GPS/Galileo precise point positioning. Coordinates.

Boehm, J. and H. Schuh (2004): *Vienna mapping functions in VLBI analyses*. Geophysical Research Letters 31(1)

Beutler G, Bock H, Fridez P, Gade A, Hugentobler U, Dach R, Jaggi A, Meindl M, Mervart L, Prange L, Schaer S, Springer T, Urschl C, Walser P (2007): *Bernese 5 GPS Software user manual*. Astronomical Institute, University of Bern

Dach R, Brockmann E, Schaer S, Meindl M, Prange L, Bock H, Jaggi A, Ostini L (2009): *GNSS processing at code: status report*. J Geodes 83:353–365

Dach R, Schmid R, Schmitz M, Thaller D, Schaer S, Lutz S, Steigenberger P, Wubbena G, Beutler G (2011): *Improved antenna phase centre models for GLONASS*. GPS Solut 15:49–65

Draper, N. R. (2002): *Applied regression analysis:bibliography update 2000-2001*. Communications in Statistics- Theory and Methods, 31(11), 2051-2075.

Deng, C., Tang, W., Liu, J. and Shi, C. (2013): *Reliable single-epoch ambiguity resolution for short baselines using combined GPS/BeiDou system*. GPS Solutions, 18(3):375-386, doi: 10.1007/s10291-013-0337-5

El-Rabbany, A. (2006): Introduction to GPS: The global positioning system. Artech House Publishing

Elsobeiey, M. and A. El-Rabbany (2010):. *On stochastic modeling of the modernized global positioning system (GPS) L2C signal*. Journal of Measurement Science and Technology, Volume 21, Number 5, pp. 1-6.

Euler, H. J. and Goad, C. G. (1991): On optimal filtering of GPS dual frequency observations without using orbit information. Bulletin Geodesique, 65:130–143

Ferrao, P. F. (2013): *Positioning with Combined GPS and GLONASS Observations*. Thesis to obtain the Master of Science Degree in Aerospace Engineering.

GPS World (2015a): *Galileo's Two Newest Birds Undergoing Initial Checks*. GPS World, March 30, 2015, http://gpsworld.com/galileos-two-newest-birds-undergoing-initial-checks/, viewed 9/5/2015

GPS World (2015b): *China Launches First of Next-Gen BeiDou Satellites*. GPS World, March 30, 2015, http://gpsworld.com/secretive-beidou-launch-unconfirmed/, viewed 9/5/2015

Habrich H (2009): Evaluation of analysis options for GLONASS observations in regional GNSS networks. Geodetic Ref Frames 134:121–129

Hofmann-Wellenhof, B. H. (2008): GNSS global navigation satellite systems; GPS, Glonass, Galileo & more. Wien New York: Springer.

He, H., Li, J., Yang, Y., Xu, J., Guo, H. and Wang, A. (2013): *Performance assessment of single- and dual-frequency BeiDou/GPS single-epoch kinematic positioning*. GPS solutions, 18(3):393- 403, doi:10.1007/s10291-013-0339-3

Ibrahim, H. E., and A. El-Rabbany (2008): *Regional stochastic models for NOAA based residual tropospheric delays*. The Journal of Navigation. 61. 209-219.

IGS - MGEX, Oliver Montenbruck , Peter Steigenberger (2014): *Preparing the ground for Multi-GNSS Constelation*. (www.insidegnss.com)

J.Sanz Subirana, J.M. Juan Zornoza and M. Hernandez-Pajares (2013): *GNSS Data Processing. Volume I. Fundamentals and Algorithms*. An ESA Communications Production.

.Kouba J, Heroux P (2001): Precise Point Positioning using IGS orbit products. GPS Solutions, 5(2): 12-28

. Langley RB (1997): GPS receiver system noise. GPS World, 8(6): 40-45

Leandro, R. F. and M. C. Santos (2007): *Stochastic models for GPS positioning: An empirical approach.* GPS World 18(2):50-56.

.Montenbruck, O., Hauschild, A., Hessels, U., Steigenberger, P., Hugentobler, U. (2009): *CONGO first GPS/Giove tracking network for science, research*. GPS World, 20(9), 56-62.

Mueller TM (1994): Wide area differenial GPS. GPS World, 5(6): 36-44

Nadarajah, N., Teunissen, P.J.G., Sleewaegen, J.M. and Montenbruck, O. (2014): *The mixed-receiver BeiDou inter-satellite-type bias and its impact on RTK positioning*. GPS Solutions, doi:10.1007/s10291-014-0392-6

Nadarajah, N., Khodabandeh, A. and Teunissen, P.J.G. (2015): Assessing the IRNSS L5-signal in combination with GPS, Galileo, and QZSS L5/E5a-signals for positioning and navigation. GPS Solutions, doi:10.1007/s10291-015-0450-8

Nadarajah, N., Khodabandeh, A. and Teunissen, P.J.G. (2015): *Assessing the IRNSS L5-signal in combination with GPS, Galileo, and QZSS L5/E5a-signals for positioning and navigation*. GPS Solutions, doi:10.1007/s10291-015-0450-8

Odijk, D. and Teunissen, P.J.G. (2013): *Characterization of between-receiver GPS-Galileo inter-system biases and their effect on mixed ambiguity resolution*. GPS Solutions, 17(4):521-533.

Odolinski, R, Teunissen, P.J.G. and Odijk, D. (2013): *Quality analysis of a combined COMPASS/BeiDou-2 and GPS RTK positioning model*. International Global Navigation Satellite Systems Society (IGNSS) Symposium, Outrigger Gold Coast, Qld Australia 16-18 July, 2013

Odolinski, R., Teunissen, P.J.G. and Odijk, D. (2014a): First combined COMPASS/BeiDou-2 and GPS positioning results in Australia. Part II: Single- and multiple-frequency single-baseline RTK positioning. Journal of Spatial Science, 59(1):25-46. doi: 10.1080/14498596.2013.866913

Odolinski, R., Teunissen, P.J.G. and Odijk, D. (2014b): *Combined GPS+BDS+Galileo+QZSS for long baseline RTK positioning*. Proceedings of the 27th International Technical Meeting of the Satellite Division of the Institute of Navigation (ION GNSS+), pp. 2326-2340. Manassas, VA: Institute of Navigation

Odolinski, R., Teunissen, P.J.G. and Odijk, D. (2015a): *Combined BDS, Galileo, QZSS and GPS single-frequency RTK*. GPS Solutions, 19:151-163. doi: 10.1007/s10291-014-0376-6

Odolinski, R., Teunissen, P.J.G. and Odijk, D. (2015b): *Combined GPS + BDS for short to long baseline RTK positioning*. Measurement Science & Technology, 26, 045801. doi: 10.1088/0957-0233/26/4/045801

Teunissen PJG (1985) Zero order design: generalized inverses, adjustment, the datum problem and S-transformations. Grafarend EK, Sanso F (eds) Optimization and design of geodetic networks. Springer, London

Teunissen P.J.G. (1995): The least squares ambiguity decorrelation adjustment: a method for fast GPS integer estimation. Journal of Geodesy 70:65-82

Teunissen P.J.G. (1998): Success probability of integer GPS ambiguity rounding and bootstrapping. Journal of Geodesy 72:606–612

Teunissen PJG (2009): Adjustment theory: an introduction. Delft University Press, Delft

Xu G (2003): GPS- theory, algorithms and aplications. Springer, Berlin Heidelberg New York

Wanninger L (1999): *The performance of virtual stations in active geodetic GPS-networks under solar maximum conditions.* Proceedings of ION GPS-99, September 14-17: 1419-1427.

Witchayangkoon B (2000): *Elements of GPS precise point positioning*. PhD Disertation, University of Maine, Orono, Maine.

Zhang, B. and Teunissen, P.J.G. (2015): Zero-baseline Analysis of GPS/BeiDou/Galileo BetweenReceiver Differential Code Biases (BR-DCBs): Time-wise Retrieval and Preliminary Characterization. Proceedings of ION 2015 Pacific PNT Meeting, Honolulu, Hawaii, April 20- 23, 2015

IGS. (2015, november, 30): MGEX. on: http://igs.org/mgex.